EBioMedicine 3 (2016) 26–42

Contents lists available at ScienceDirect

EBioMedicine

journal homepage: www.ebiomedicine.com

Research Paper

Amelioration of Metabolic Syndrome-Associated Cognitive Impairments in Mice via a Reduction in Dietary Fat Content or Infusion of Non-Diabetic Plasma

Lance A. Johnson [a], Kristen L. Zuloaga [b], Tara L. Kugelman [a], Kevin S. Mader [c,d], Jeff T. Morré [e], Damian G. Zuloaga [a], Sydney Weber [a], Tessa Marzulla [a], Amelia Mulford [a], Dana Button [a], Jonathan R. Lindner [f], Nabil J. Alkayed [b,f], Jan F. Stevens [e], Jacob Raber [a,g,*]

[a] Department of Behavioral Neuroscience, Oregon Health & Science University, Portland, OR 97239, USA
[b] Department of Anesthesiology and Perioperative Medicine, Oregon Health & Science University, Portland, OR 97239, USA
[c] Swiss Federal Institute of Technology, Zurich, Switzerland
[d] 4Quant, Paul Scherrer Institute, Villigen, Switzerland
[e] Department of Pharmaceutical Sciences, and the Linus Pauling Institute, Oregon State University, Corvallis, OR 97331, USA
[f] Knight Cardiovascular Institute, Oregon Health & Science University, Portland, OR 97239, USA
[g] Departments of Neurology and Radiation Medicine, Division of Neuroscience, ONPRC

ARTICLE INFO

Article history:
Received 1 October 2015
Received in revised form 26 November 2015
Accepted 11 December 2015
Available online 12 December 2015

Keywords:
Obesity
Metabolic syndrome
Diabetes
Brain
Cognitive
Cerebrovascular
Plasma

ABSTRACT

Obesity, metabolic syndrome (MetS) and type 2 diabetes (T2D) are associated with decreased cognitive function. While weight loss and T2D remission result in improvements in metabolism and vascular function, it is less clear if these benefits extend to cognitive performance. Here, we highlight the malleable nature of MetS-associated cognitive dysfunction using a mouse model of high fat diet (HFD)-induced MetS. While learning and memory was generally unaffected in mice with type 1 diabetes (T1D), multiple cognitive impairments were associated with MetS, including deficits in novel object recognition, cued fear memory, and spatial learning and memory. However, a brief reduction in dietary fat content in chronic HFD-fed mice led to a complete rescue of cognitive function. Cerebral blood volume (CBV), a measure of vascular perfusion, was decreased during MetS, was associated with long term memory, and recovered following the intervention. Finally, repeated infusion of plasma collected from age-matched, low fat diet-fed mice improved memory in HFD mice, and was associated with a distinct metabolic profile. Thus, the cognitive dysfunction accompanying MetS appears to be amenable to treatment, related to cerebrovascular function, and mitigated by systemic factors.

1. Introduction

Diabetes has reached epidemic proportions, and projected rates predict that nearly 600 million people throughout the world will have diabetes within the next 20 years (Guariguata et al., 2014). Type 2 Diabetes (T2D), characterized by obesity and insulin resistance (IR), accounts for over 90% of all diabetes incidence (Engelgau et al., 2004). Aside from traditional complications, T2D poses an additional health risk in the form of cognitive decline and dementia. While learning and memory is generally unaffected during type 1 diabetes (T1D) (Brands et al., 2005), individuals with T2D often demonstrate multiple cognitive impairments (Kodl and Seaquist, 2008) and their risk of developing dementia is significantly increased compared to non-diabetic individuals (Cheng et al., 2012). Furthermore, obesity, IR and metabolic syndrome (MetS) are also associated with decreased cognitive function and an increased risk of dementia even in the absence of overt diabetes (Baker et al.,

Abbreviations: ADMA, Asymmetric dimethylarginine; BW, Body weight; BDNF, Brain-derived neurotrophic factor; Br Fat, Brown adipose tissue; CBV, Cerebral blood volume; C-X-C motif, Chemokine; Cxcl1, Ligand 1; CH, Cholesterol; DG, Diacylglycerol; FFA, Free fatty acids; GLP-1, Glucagon-like peptide 1; GlcCer, Glucosylceramide; HFD, High fat diet; GL, Glycerolipid; GPL, Glycerophospholipid; IR, Insulin resistance; ITT, Insulin tolerance test; IFNγ, Interferon-γ; Il-1b, Interleukin-1β; IL-6, Interleukin-6; IL-10, Interleukin-10; IL-12p70, Interleukin-12p70; LFD, Low fat diet; LPA, Lysophosphatidic acid; MetS, Metabolic syndrome; OGTT, Oral glucose tolerance test; PC, Phosphatidylcholine; PE, Phosphatidylethanolamine; PG, Phosphatidylglycerol; PGP, Phosphatidylglycerolphosphate; PI, Phosphatidylinositol; PS, Phosphatidylserine; SC Fat, Subcutaneous adipose tissue; KB, Total ketone bodies; TG, Triglycerides; TNFα, Tumor necrosis factor-α; T1D, Type 1 Diabetes; T2D, Type 2 Diabetes; V Fat, Visceral adipose tissue.

* Corresponding author at: Department of Behavioral Neuroscience, Oregon Health & Science University, Portland, OR 97239, USA.
E-mail address: raberj@ohsu.edu (J. Raber).

http://dx.doi.org/10.1016/j.ebiom.2015.12.008

2011; Gunstad et al., 2010; Kim and Feldman, 2015; Matsuzaki et al., 2010; Schrijvers et al., 2010).

Sedentary lifestyle and caloric excess are the primary contributors to obesity, which in turn is the major modifiable risk factor for MetS and T2D (Ershow, 2009). Thus, diet-induced obesity comprises a critical risk factor for the development of cognitive impairment. Weight loss is associated with improvements in general metabolism, vascular function and cardiovascular mortality (Bigornia et al., 2010; Sjöström et al., 2012). While less clear, evidence suggests that the benefits of weight loss may also extend to cognitive performance (Espeland et al., 2014) and the risk of developing dementia (Siervo et al., 2011). In addition to an inverse association between IR and memory, a possible association between improved insulin sensitivity and improved cognition would suggest that IR plays an important role during cognitive decline (Brinkworth et al., 2009; Witte et al., 2009). Thus, lifestyle changes such as weight loss may represent an effective therapeutic approach to preventing or ameliorating cognitive decline due to their established benefits on insulin sensitivity and endothelial function (Blumenthal et al., 2010; Mavri et al., 2011; Rudofsky et al., 2011). However, controlled long-term studies in humans are challenging, and the mechanisms of action remain undetermined.

While the precise biological mechanisms by which obesity and weight loss affect cognitive function are unclear, several plausible pathways exist, including oxidative stress, inflammation, metabolic impairments and vascular dysfunction (Bruce-Keller et al., 2009). Of these potential mechanisms, cerebrovascular function represents an intriguing potential link between diabetes and cognition, as individuals with T2D show deficits in the maintenance and regulation of cerebral blood flow (CBF) compared to non-diabetic controls (Kim et al., 2008; Novak et al., 2006).

Multiple studies have demonstrated varying neurobiological deficits and cognitive impairments in rodent models of obesity, IR and diabetes (Gault et al., 2010; Li et al., 2002; Stranahan et al., 2008a, 2008b; Winocur et al., 2005). In the present study, we employed a commonly used mouse model of chronic high fat diet (HFD) consumption in order to assess whether the cognitive impairments associated with MetS can be mitigated. The prevalence of cognitive impairment is higher in women (Hebert et al., 2013), and while age is the strongest risk factor for cognitive decline and dementia, it has become increasingly clear that cognitive decline in late life is due in large part to vascular risk factors such as diabetes during middle age (Debette et al., 2011). Therefore, we induced MetS through chronic administration of a HFD in "middle aged" female mice and analyzed the metabolic, cognitive and cerebrovascular effects of MetS during old age. We then tested the restorative potential of weight loss and improvements in peripheral metabolism on cerebrovascular function and cognition by reducing the dietary fat content in HFD-fed mice over a one month period.

Given the established peripheral vascular impairments associated with T2D and the importance of cerebrovascular function for cognition, it is plausible that circulating factors could affect brain function during T2D. In fact, past studies involving shared circulations suggest that systemic factors can modulate obesity and T2D (Coleman, 2010). Additionally, there has been increased interest in the role of systemic factors in modulating health during old age, as a series of studies have shown that young blood has numerous rejuvenating properties (Loffredo et al., 2013; Ruckh et al., 2012; Salpeter et al., 2013). These studies strongly suggest that factors present in a young systemic circulation are able to reverse certain aspects of aging, including brain function (Katsimpardi et al., 2014; Villeda et al., 2014). For example, exposure to young blood enhanced neuronal spine density and synaptic plasticity (Villeda et al., 2014) and induced vascular remodeling and neurogenesis (Katsimpardi et al., 2014) in old mice. Additionally, pancreatic beta cells exposed to a young systemic circulation demonstrate increased replication (Salpeter et al., 2013). To date, these experiments have all focused on aging and age differences between donors and recipients, and the therapeutic capacity of systemic factors has yet to be explored in the context of specific disease states and age-matched donors and recipients. Therefore, to assess whether similar cognitive benefits extend beyond aging to the context of MetS, we tested the hypothesis that repeated infusion of "healthy" plasma collected from age-matched, low fat diet (LFD)-fed mice could improve cognitive function in mice with MetS.

2. Materials and Methods

2.1. Experimental Animals and Diet

Wild type female mice on a C57BL/6 background (Jackson Labs) were employed in this study. Female mice were used as the prevalence of cognitive impairment is higher in women (Hebert et al., 2013). Additionally, vascular risk factors during middle age drive development of dementia in later life (Debette et al., 2011). Therefore, mice were fed a specialized diet beginning at 9 months of age, and metabolic and cognitive analyses were carried out at 14 and/or 15 months of age. T1D was induced by five days of sequential intraperitoneal low-dose streptozotocin (STZ) injections, at 12 months of age, as described (Johnson et al., 2011). Obesity and MetS were induced by administration of a high fat diet (HFD) (60% kcal from fat, Research Diets D12492, New Brunswick, NJ, USA). Control mice (and T1D mice) were fed an ingredient-matched low fat diet (LFD) (10% kcal from fat, Research Diets D12450B). The constituent components of the employed diets are shown as follows (Ingredient (grams in HFD; grams in LFD)): Casein (200; 200), L-cystine (3; 3), corn starch (0; 315), maltodextrin 10 (125; 35), sucrose (68; 350), cellulose BW200 (50; 50), soybean oil (25; 25), lard (245; 20), mineral mix S10026 (10; 10), di-calcium phosphate (13; 13), calcium carbonate (5.5; 5.5), potassium citrate (16.5; 16.5), vitamin mix V10001 (10; 10), choline bitartrate (2; 2) and FD&C dye #1 (blue 0.05; yellow 0.05). Metabolic and behavioral measures (with the exception of the water maze involving multiple platform locations) were completed in one cohort of mice, while a second cohort was employed for the water maze involving multiple platform locations and cerebral blood volume measures, and a final cohort employed for the plasma infusion studies. All mice were housed on a 12 hour light/dark cycle (5:00 AM–5:00 PM). Plasma samples for fasting metabolic measures were taken at ~1:00 PM following a four hour fast. Periods of 4 to 6 h of fasting are considered to be adequate for a definition of fasting in mice as it avoids massive reduction in body fat content and glycogen stores (Mutel et al., 2011; Pacini et al., 2013). Behavioral tests were typically assessed beginning at ~9:00 AM. For adipose tissue measurements, the left epididymal fat pad (visceral) and left inguinal fat pad (subcutaneous) were weighed. All procedures complied with the National Institutes of Health Guide for the Care and Use of Laboratory Animals and with IACUC approval at Oregon Health & Sciences University.

2.2. Biochemical Measurements

For the glucose tolerance test, mice were administered an oral gavage of glucose solution (2 mg/g body weight). For the insulin tolerance test, mice were intravenously injected with 0.75 U/kg of human insulin (Gibco). Blood glucose was measured using a glucometer (One Touch Ultra) at indicated time points. Plasma triglycerides (Cayman Chemicals), free fatty acids (ZenBio), glucose, total cholesterol and ketone bodies (Wako), and plasma insulin (Millipore) were measured following a four-hour fast. GLP-1 was measured using a commercial ELISA (RayBioTech). Plasma protein levels of interferon-γ, interleukin-1β, interleukin-6, KC/GRO (Cxcl1), interleukin-10, interleukin-12p70 and tumor necrosis factor-α were assessed in a sandwich immunoassay format (7-Plex assay kit) according to the manufacturer's instructions (MesoScale Discovery). For glucose uptake, mice were injected following a four hour fast with 0.75 μCi of 2-[1,2-^{3}H (N)]-deoxy-D-glucose (Perkin Elmer), diluted in 100 μl of 0.25 g/ml glucose solution, via the tail vein. Twenty minutes after injection, mice were intraperitoneally administered a lethal dose of

ketamine–xylazine–acepromazine cocktail (0.01 ml/g of 25 mg/ml ketamine (Sigma), 0.625 mg/ml acepromazine (Vetus Animal Health), 3.125 mg/ml xylazine (Sigma)), intracardially perfused with 20 ml of 0.9% Phosphate-Buffered Saline (PBS), and tissues were collected. For tissue glucose uptake, 25–150 mg of tissue was homogenized in 4 ml of PBS. The following tissues were collected for glucose uptake: brain (cortex), skeletal muscle (right quadriceps), liver (median lobe), visceral fat (right epididymal pad), subcutaneous fat (right inguinal pad), and brown adipose tissue (interscapular). Homogenates were transferred to a scintillation vial, 1 ml of Optiphase scintillation fluid (Perkin Elmer) was added, and samples were measured on a liquid scintillation counter (Beckman).

2.3. Behavioral and Cognitive Analyses

2.3.1. Activity Monitoring and Nest Building

Activity was monitored using infrared home-cage activity sensors (Biobserve, St. Augustin, Germany). Mice were individually housed and acclimated to the home-cage environment for three days prior to activity monitoring. Activity counts (beam breaks) were measured every second for two weeks and data were expressed as mean activity count per hour. Nest building was measured using an established protocol (Deacon, 2006). Briefly, mice were individually housed in a clean cage and provided two pressed cotton squares (Ancare, Bellmore, NY). Photos of the home cage were taken 48 h later and visually rated by four different blinded scorers on a 5-point nest rating scale.

2.3.2. Anxiety-Like Behavior

Exploratory and anxiety-like behaviors were assessed using the open-field. The open-field consisted of a brightly lit square arena (L 40.6 × W 40.6 × H 40.6 cm). The light intensity in the center of the open field was 100 lux. Mice were allowed to explore for 10 min. Behavioral performance was tracked and scored using an automated video system (Ethovision 7.0 XT, Noldus). Exploratory behavior was analyzed using total distance moved, and time spent in the more anxiety-provoking center (10 × 10 cm) of the open field was also analyzed.

2.3.3. Novel Object Recognition

Mice were placed into the square arena used during the open-field testing, and habituated to the open field arena over two days, with one 10-minute trial per day. On the third day, mice were exposed to the arena containing two identical objects (small orange hexagonal prisms) placed 15 cm from the adjacent walls and 10 cm apart for 15 min. On day four, one of the identical objects ("familiar") was replaced with a novel object (small green triangular prism) of identical dimensions. During the open-field and novel object recognition tests, mice were placed into the arena at varying locations during each trial, and the location of the novel object was randomized to avoid procedural bias. Clear visuospatial orientation to the object, within 2 cm proximity, as well as physical interaction with the object was coded as exploratory behavior, and the percent time spent exploring the novel versus familiar object was calculated.

2.3.4. Spatial Learning and Memory in the Water Maze

The water maze consisted of a circular pool (diameter 140 cm), filled with opaque water (white chalk added, 24 °C) divided conceptually into four quadrants. Mice were given two sessions per day (separated by three hours) consisting of two trials each (separated by 5 min), over the course of five days (2 days "Visible Platform" followed by 3 days "Hidden Platform"). Mice were first trained to locate an "escape" platform (Plexiglas circle, 6 cm radius) submerged 2 cm below the surface of the water, by the use of a cue (a colored cylinder, 2.5 cm radius, 8 cm height) during the "Visible Platform" trials. Mice were removed from the pool after locating the platform and remaining on it for 3 s. Mice were inserted in the maze at varying locations during each trial to avoid procedural bias, and during the Visible Platform trials, the location of the platform was moved for each session between the four quadrants to avoid procedural biases in task learning. Subsequent to the "Visible Platform" trials, mice were trained to locate the platform sans cue during the "Hidden Platform" trials, which required the mice to rely on extra-maze cues for spatial reference and orientation. Extra-maze cues consisted of four large (50 × 50 cm) cues of different shapes and color combinations, positioned at the borders of the four quadrants. The platform was not rotated during the Hidden Platform trials, remaining in the "Target" quadrant. Spatial memory retention was assessed 24 h following the conclusion of the fourth session of "Hidden Platform" training, as well as 72 h following the final "Hidden Platform" training session. The submerged platform was removed and spatial memory retention assessed during these "Probe" trials by calculating the cumulative distance from the target.

2.3.5. Spatial Learning and Memory in the Water Maze (Varied Platform Locations)

Following five months of diet, mice were given three days of spatial memory water maze testing similar to as described above. However, in this protocol, the location of the platform was changed daily. Mice were given two sessions per day (separated by three hours) consisting of two trials each (separated by 5 min). Upon completion of the first three days of testing, a randomly assigned subset of HFD mice was switched to a low fat diet. One month later, all mice were re-tested using the same protocol described above, with three new hidden platform locations. For plasma infusion experiments, the same experimental design was followed, except in this case the mice received one day of baseline testing followed by multiple plasma infusions and two additional testing days with new hidden platform locations.

2.3.6. Fear Learning and Cued Fear Memory

In this task, mice learned to associate a conditioned stimulus (CS, e.g. the environmental context, or a discrete cue — tone) with a mild foot shock (unconditioned stimulus, US). Freezing, defined as somatomotor immobility with the exception of respiration, is considered a post-exposure fear response, and is a widely used indicator of conditioned fear (Maren, 2001). Mice were trained and tested using a Med Associates mouse fear conditioning system (PMED-VFC-NIR-M, Med Associates, St. Albans, Vermont) utilizing Med Associates VideoFreeze automated scoring system. Mice were placed inside the fear conditioning chamber, and chamber lights were turned on at zero seconds, followed by a 160 second habituation period and a subsequent 30-second (80 dB) tone (cue). A 2-second 0.35 mA foot shock was administered at 188 s, co-terminating with the tone at 190 s. This series was repeated for a total of four times. Twenty-four hours later, mice were exposed to a modified environment (scented with vanilla extract, novel floor texture covering the shock-grid, and rounded walls), allowed to habituate to it for 160 s, and were then exposed to the sound cue for a second period of 30 s. This series was repeated a total of four times. Motion during shock during the training day was measured to account for sensor–motor differences in response to the aversive stimulus. Cued fear memory was determined as the percent time spent freezing in response to the tone (cue).

2.4. Cerebral Blood Volume (CBV), Vascular Casting and Vessel Analyses

To monitor changes in vessel diameter and vascular perfusion (volume of blood-perfused vessels, referred to as cerebral blood volume (CBV) throughout the manuscript) *in vivo*, we used optical microangiography (OMAG), an imaging technique based on optical coherence tomography (OCT) (Jia et al., 2011). We used OMAG because it allows for *in vivo*, high-resolution, non-invasive quantification of CBV in mouse brain through an intact skull in real time (Jia et al., 2009). CBV was calculated based on endogenous light scattering from moving blood cells within brain vessels. Briefly, mice were

anesthetized with isoflurane and body temperature was maintained at 37 ± 0.5 °C using a warm water pad. The skin over the skull was reflected, the cortex illuminated through the skull at 1310 nm, and the resulting backscattered and reference light detected to produce spectral interferograms. A final volume data cube is constructed from which the three-dimensional OMAG structural and flow images are computed. In our study, volumetric imaging data were collected by scanning the probe beam through a 1000 × 500 × 512-voxel cube, representing 2.5 × 2.5 × 2 mm^3 (x–y–z) of tissue. Corresponding OMAG images of the same area of the brain (branch of the middle cerebral artery) were aligned for quantification of CBV before and after the intervention, as previously described (Siler et al., 2015). OMAG images were rendered in the 3-D software AMIRA (FEI) and analyzed for mean pixel intensity changes over time using ImageJ. For vessel diameter measurements, average vessel diameters were measured for each branching segment of the MCA within the scan area, and pixel intensity histograms were generated using ImageJ.

For vascular casting, mice were deeply anesthetized with a ketamine–xylazine–acepromazine cocktail and immediately perfused through the left ventricle at 4 ml/min, first with 20 ml PBS containing heparin (25 U/ml), followed by 20 ml 4% formalin in PBS, followed by 5 ml of the polyurethane PU4ii (vasQtec, Zurich, Switzerland). The characteristics of this casting material have previously been described in detail (Krucker et al., 2006). Brains were immediately removed and cured in 4% formalin for 48 h and then transferred to 30% sucrose for 48 h. Casted brains were then coronally sectioned at 50 μm into two series using a cryostat (Microm HM505E, MICROM International GmbH, Walldorf, Germany). Images were taken at 10× magnification using an Olympus IX81 confocal microscope equipped with Slidebook software (3i, Ringsby, CT, USA). Vessel territories analyzed include areas ranging from 500 μm rostral and 500 μm caudal of Bregma 1.94 mm (prefrontal cortex) or Bregma −1.82 (hippocampus). Z-stack images taken within these areas represented a 3D area of analysis with the following dimensions: 2.56 × 0.65 × 1.0 mm. Vessel diameter and volume were analyzed using 4Quant (Zurich, Switzerland) and Amira (FEI, Houston, TX, USA) software. For analyses designed by 4Quant, a Gaussian filter and threshold were applied to all images and several morphological operations were used to remove spurious voxels and better connect the structures. Physically contiguous vessels were identified with component labeling on the segmented image. The main regions of the network were extracted and a thickness analysis was performed by fitting the largest sphere in each portion of the vessel which then corresponds to its local diameter, similar to previously described (Hildebrand and Rüegsegger, 1997). From the thickness map, a ridge was identified which shows the skeleton of the vessel network, which was then labeled and regrown into the original structure. The densities corresponding to various regions and vessel diameters were then calculated from the territories of the Voronoi Tessellation. For analyses performed using Amira software, mean vessel diameter, volume and branching were measured using the proprietary XSkeleton feature.

2.5. Plasma Infusion and Metabolomics

Blood was collected from 34–50 female mice ("donor mice"), 15 months of age, into EDTA-coated tubes at time of death. Beginning at 9 months of age, donor mice were administered either a high fat or low-fat diet for 6 months prior to plasma collection. Recipient T2D mice were 15 month old female mice, as described above. Plasma was generated by centrifugation (3000× *g*, 10 min at 4 °C) of freshly collected blood and aliquots were stored at −80 °C until use. Prior to administration, plasma was pooled and dialyzed in PBS overnight at 4 °C using 3.5-kDa D-tube dialyzers (EMD Millipore) to remove EDTA, as described (Villeda et al., 2014). Mice were systemically treated with plasma (100 μl per injection) via intravenous injection five times over the course of 10 days (injected every other day at ~8:30 AM). Injections and cognitive testing were carried out by investigators blinded to treatment groups.

The untargeted metabolomics analysis was performed on plasma samples collected from HFD recipient mice 24 h following repeated infusion of donor plasma and completion of cognitive testing. Unbiased metabolomics profiling was completed as previously described with minor changes (Kirkwood et al., 2013). Briefly, liquid chromatography (LC) was performed on a Shimadzu Nexera system with a phenyl-3 stationary phase (Inertsil Phenyl-3, 4.6 × 150 mm, Phenomenex, Torrance, CA) coupled to a quadrupole time-of-flight mass spectrometer (Q-TOF) (AB SCIEX, Triple TOF 5600) operated in information dependent MS/MS acquisition mode. Samples were ordered randomly, including multiple quality control samples, and automatic mass calibrations were performed every hour. Samples were run in positive and negative ion modes. Column temperature was held at 50 °C and samples at 10 °C.

Untargeted metabolomics data was processed using MarkerView and Peakview software (AB SCIEX) and the web-based metabolomic data processing tool Metaboanalyst (Xia and Wishart, 2011). Significant metabolites were defined by a Student's *t*-test and subsequent *p*-value cutoff ($p < 0.05$). Metabolite identification was based on mass error, MS/MS fragment ions, and when possible comparison to an authentic standard retention time. LipidView software (AB Sciex) and the online LipidMaps, METLIN and Human Metabolome Database (HMDB) metabolite databases were used for MS and MS/MS matching. Many metabolites were further confirmed with retention time by comparison to authentic standards from an in-house library containing 619 metabolite standards (IROA Technologies, Bolton, MA). For hierarchical clustering, pathway impact and random forest analyses, the online tool Metaboanalyst was used. For pathway impact and random forest analyses, all 298 identified metabolites were included. For heatmap analysis, only significantly altered features were analyzed and data was organized using a Euclidean distance map and complete clustering algorithm. For random forest and pathway impact analyses, data were filtered using the interquantile range (IQR) function and scaled using auto-scaling, in which values are mean-centered and divided by the standard deviation of each variable. For the random forest analysis, the number of predictors to try for each node was set to the square root of the total number of variables and the number of trees to grow was set to 5000. For the pathway impact analysis, the parameters were set to 'global test' and 'Relative Betweenness Centrality', a node centrality measure which reflects metabolic pathway 'hub' importance.

2.6. Statistical Analyses

Data are expressed as mean ± standard error. Multiple groups and/or multiple time points were analyzed using one-way ANOVA (groups = HFD, LFD, and HFD–LFD) using Graph Pad Prism (San Diego, CA), or repeated measures ANOVA (time × groups) using SPSS software (Chicago, IL). To assess potential correlations, two-tailed Pearson correlations were generated using GraphPad Prism software. For correlation matrices, Pearson's r rank correlation coefficients were computed using z-score transformed values. Statistically significant correlations were determined using an error probability level of $p < 0.05$ corrected by a false discovery rate (FDR) analysis.

3. Results

3.1. HFD-Induced MetS; Weight Loss and Improvements in Metabolism Following a Reduction in Dietary Fat Content

To model the progression of obesity, insulin resistance (IR) and metabolic syndrome (MetS), mice were fed a high fat diet (HFD) over the course of six months. To test the restorative potential of weight loss, a subset of HFD mice were administered a one month reduction in dietary fat content following five months of HFD (hereafter referred to as HFD–LFD) (Fig. 1A). Substantial group differences in body weight ($F_{(2,23)} = 7.263$, $p = 0.004$, repeated measures ANOVA), visceral

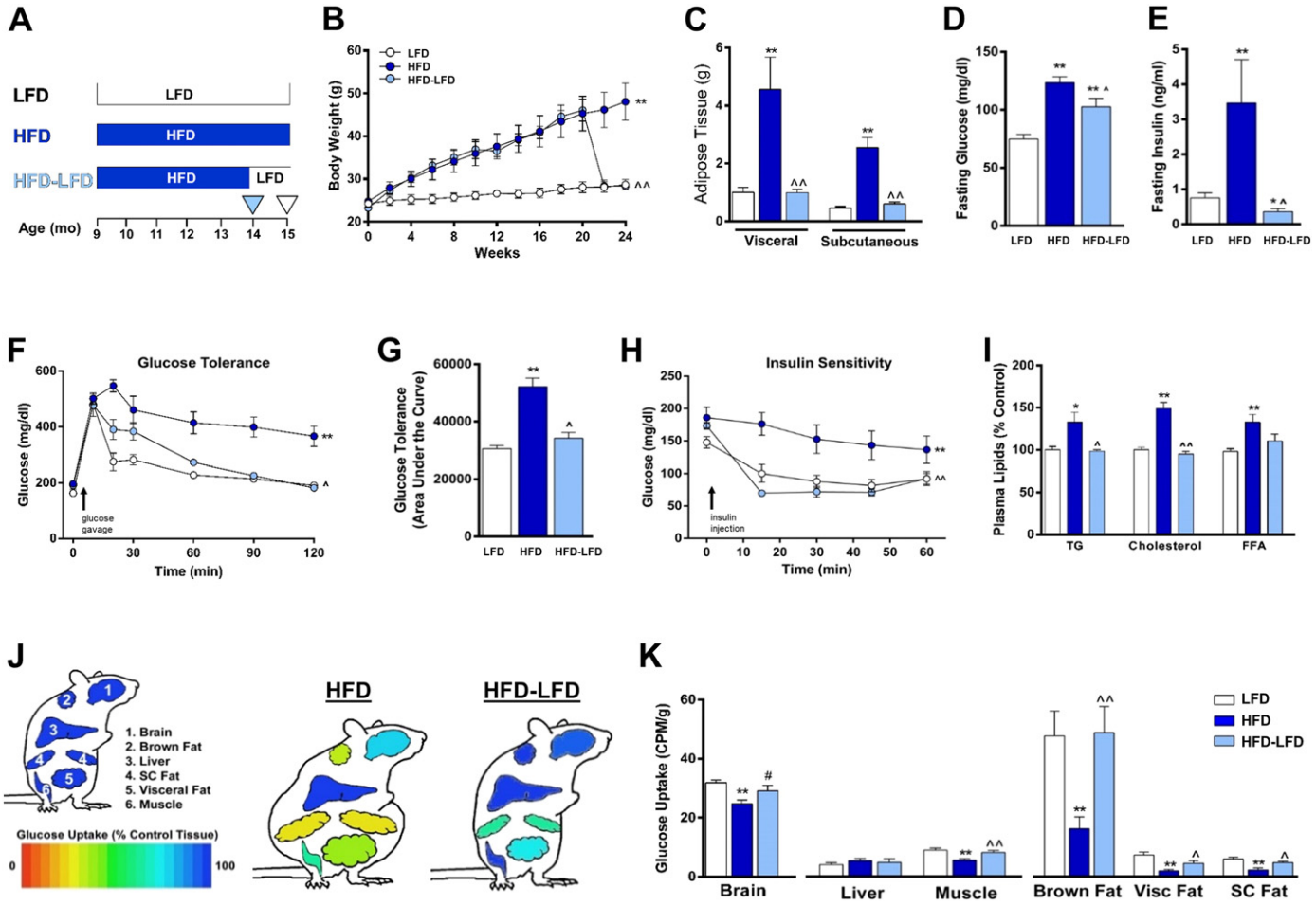

Fig. 1. HFD-Induced MetS; Restoration of Metabolism via a Short-Term Reduction in Dietary Fat Content. (A) Experimental Design. MetS was induced in "middle aged" mice (9 months) via administration of a high fat diet (HFD) for 6 months. A subset of HFD mice were given an intervention ("HFD–LFD") by switching to an ingredient-matched low fat diet (LFD) at 14 months of age (light blue triangle). Behavioral testing, cerebrovascular imaging, and biochemical analyses were carried out at 14 and 15 months of age (white triangle). (B) Mice fed a high fat diet become obese; HFD–LFD mice lose substantial body weight following a reduction in dietary fat content (week 20). Body weight was measured bi-weekly over the course of diet administration. (C) HFD mice gain adipose tissue mass; fat loss following a reduction in dietary fat content. Adipose tissue weight was measured from the left visceral (gonadal) and left subcutaneous (inguinal) fat pads. (D–E) Glucose and insulin are elevated during MetS and reduced following a reduction in dietary fat content. Plasma glucose and insulin were measured following a four hour fast. (F–G) Chronic HFD consumption impairs glucose tolerance; improvement following the reduction in dietary fat content. (F) Blood glucose was serially measured following an oral gavage of glucose and (G) area under the curve (AUC) was calculated. (H) Insulin sensitivity is decreased in HFD mice and improves following a reduction in dietary fat content. Blood glucose was serially measured after an intraperitoneal injection of insulin. (I) Diabetic dyslipidemia during MetS; reduced plasma lipids following the diet intervention. Plasma triglycerides (TG), cholesterol, and free fatty acids (FFA) were measured following a four hour fast. (J–K) Brain and peripheral tissue glucose uptake is reduced during MetS. Uptake of [^{3}H] 2-deoxyglucose was measured 20 min following intravenous injection. Heat maps (J) showing uptake in various organs. Colors represent group mean glucose uptake as a percent of LFD controls. (K) Total [^{3}H] 2-deoxyglucose uptake in counts per minute (CPM) per gram of tissue. $^*p < 0.05$, $^{**}p < 0.01$ compared to LFD, $^{\wedge}p < 0.05$, $^{\wedge\wedge}p < 0.01$, $^{\#}p = 0.066$ compared to HFD, ANOVA, followed by Tukey's multiple comparison test. (*B*, *F*, *H* repeated measures ANOVA). (*C–K*, measurements taken at 15 months of age). (*B*, n = 6–11; *C–D*, n = 10–15; *E–K*, *n* = 5–9).

adipose tissue mass ($F_{(2,35)} = 9.373$, $p < 0.001$, ANOVA), and subcutaneous adipose tissue mass ($F_{(2,35)} = 31.81$, $p < 0.001$, ANOVA) were observed over the course of the study (Fig. 1B–C). Following the reduction in dietary fat content, HFD–LFD mice showed considerable decreases in body weight (weeks 22–24, $F_{(2,23)} = 12.452$, $p = 0.002$, repeated measures ANOVA), and visceral (HFD vs HFD–LFD, $p = 0.003$, Tukey's multiple comparisons test (Tmct)) and subcutaneous adipose tissue mass (HFD vs HFD–LFD, $p < 0.001$, Tmct), compared to HFD mice (Fig. 1B–C). The substantial weight loss in HFD–LFD mice appeared to be a result of decreased caloric intake (Fig. 2A) ($F_{(2,37)} = 14.42$, $p < 0.001$, ANOVA; HFD vs HFD–LFD, $p < 0.001$, Tmct) rather than reduced food consumption (Fig. 2B) ($F_{(2,36)} = 0.694$, $p = 0.506$, ANOVA) or increased activity (Fig. 2C–F). Although HFD mice showed significantly reduced activity compared to LFD mice ($F_{(2,10)} = 6.758$, $p = 0.0139$, ANOVA; HFD vs LFD, $p = 0.013$, Tmct), total activity during the active (dark) cycle did not significantly differ between HFD and HFD–LFD mice following the reduction in dietary fat content (Fig. 2C–F) ($p = 0.503$, Tmct).

HFD mice demonstrated several hallmarks of MetS, all of which significantly improved following the reduction in dietary fat content (Fig. 1D–I), including hyperglycemia ($F_{(2,38)} = 21.19$, $p < 0.001$, ANOVA; HFD vs HFD–LFD, $p = 0.033$, Tmct), hyperinsulinemia ($F_{(2,22)} = 4.745$, $p = 0.0194$, ANOVA; HFD vs HFD–LFD, $p = 0.031$, Tmct), impaired glucose tolerance ($F_{(2,18)} = 17.843$, $p < 0.001$, repeated measures ANOVA; HFD vs HFD–LFD, $p = 0.002$, Tmct), decreased insulin sensitivity ($F_{(2,18)} = 6.579$, $p = 0.007$, repeated measures ANOVA; HFD vs HFD–LFD, $p = 0.019$, Tmct), and dyslipidemia (triglycerides, $F_{(2,20)} = 5.978$, $p = 0.009$; HFD vs HFD–LFD, $p = 0.032$, Tmct; cholesterol ($F_{(2,20)} = 35.96$, $p < 0.001$; HFD vs HFD–LFD, $p < 0.001$). Measures of glucose metabolism, adiposity, and dyslipidemia positively correlated with one another. Glucose uptake in various tissues positively correlated with one another, and negatively correlated with measures of glucose metabolism, plasma lipids, and degree of adiposity (Fig. 3). Although plasma glucose concentrations were lower in HFD–LFD compared to HFD mice, they remained significantly elevated compared to LFD mice (LFD vs HFD–LFD, $p = 0.003$, Tmct), while insulin levels

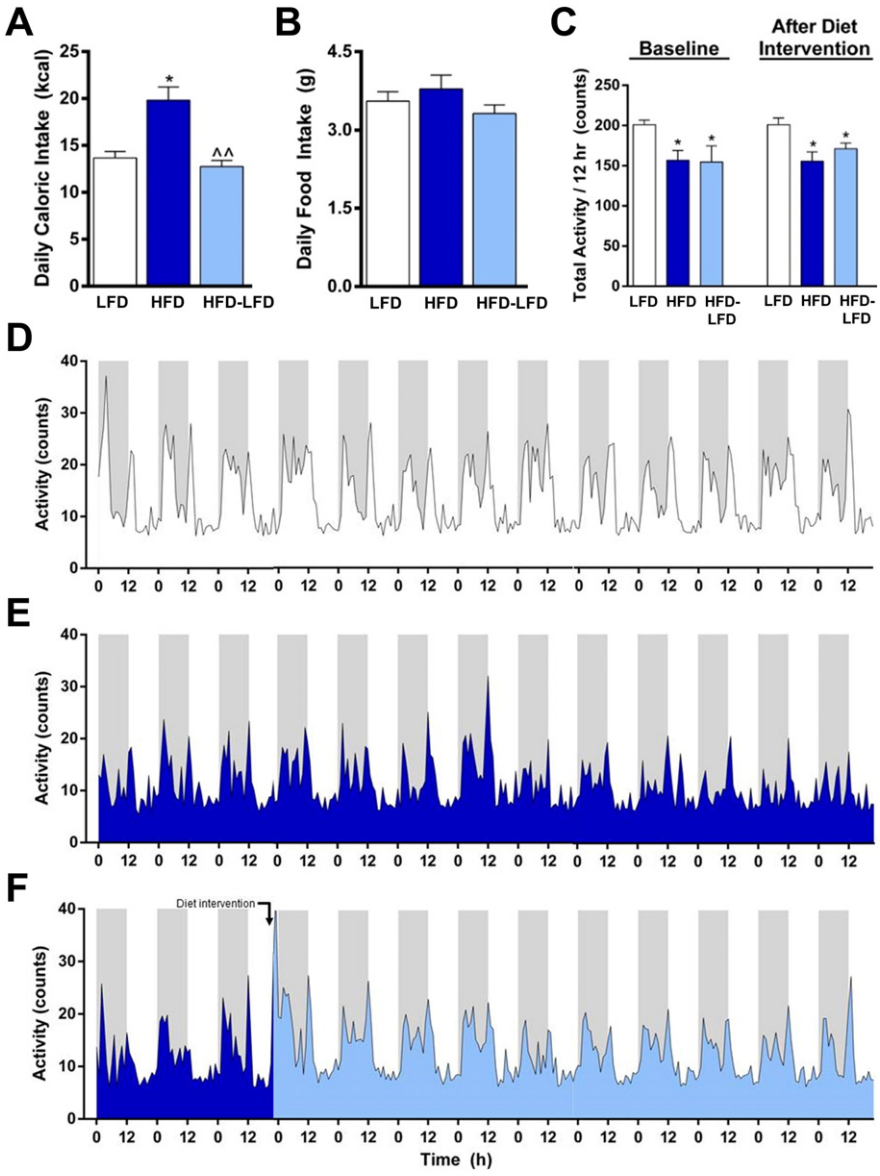

Fig. 2. Caloric Intake is Reduced in HFD–LFD Mice; HFD and HFD–LFD Mice Are Less Active. (A–B) Caloric intake is reduced in HFD–LFD mice despite a similar per gram daily food intake. (A) Total daily caloric intake (kcal) was calculated based on daily food intake. (B) Food intake was measured for four days immediately following the diet intervention. (C–F) Home cage activity is reduced in HFD and HFD–LFD mice. (C) Total activity was calculated as the mean area under the curve during the 12 hour active (dark) cycle. (D–F) Mean activity patterns of (D) control, (E) HFD and (F) HFD–LFD mice. Individually housed mice were monitored using infrared sensors for three days prior, and ten days after, the reduction in dietary fat content. $^{*}p < 0.05$, $^{**}p < 0.01$ compared to LFD, $^{\wedge}p < 0.05$, $^{\wedge\wedge}p < 0.01$ compared to HFD, ANOVA, followed by Tukey's multiple comparison test. (*A–B*, n = 11–15) (*C–F*, $n = 4–5$).

were slightly lower (LFD vs HFD–LFD, $p = 0.048$, Tmct), suggesting some lasting deficiencies in metabolism (Fig. 1D–E). HFD mice also displayed a pattern of reduced glucose uptake in the brain ($F_{(2,21)} = 7.482$, $p = 0.004$, ANOVA), as well as in several peripheral organs (Fig. 1J–K) including skeletal muscle ($F_{(2,21)} = 9.117$, $p = 0.0013$, ANOVA), visceral adipose tissue ($F_{(2,21)} = 13.32$, $p < 0.001$, ANOVA), subcutaneous adipose tissue ($F_{(2,21)} = 9.237$, $p = 0.001$, ANOVA), and brown adipose tissue ($F_{(2,21)} = 6.825$, $p = 0.005$, ANOVA). Following the reduction in dietary fat content, fasting glucose uptake significantly increased in skeletal muscle (LFD vs HFD–LFD, $p = 0.018$, Tmct), visceral adipose (LFD vs HFD–LFD, $p = 0.011$, Tmct), subcutaneous adipose (LFD vs HFD–LFD, $p = 0.014$, Tmct), and brown adipose tissue (LFD vs HFD–LFD, $p = 0.0135$, Tmct) (Fig. 1J–K). In the brain, there was a trend towards increased glucose uptake in HFD–LFD compared to HFD mice, but this did not reach significance (Fig. 1K) (HFD vs HFD–LFD, $p = 0.066$, Tmct).

Inflammation has been proposed as a possible causative link between diabetes and cognitive dysfunction (Chung et al., 2015; Novak et al., 2011). Circulating concentrations of the several critical inflammatory markers, including IL-12p70, IL1β, TNFα, and IFNγ — while generally increased in HFD mice, did not significantly differ from LFD controls or the intervention group (Table 1). However, plasma CXCL1 levels were significantly increased in HFD compared to LFD mice ($F_{(2,19)} = 9.776$, $p = 0.001$, ANOVA; HFD vs LFD, $p = 0.002$, Tmct), while HFD–LFD mice showed significantly lower concentrations of both CXCL1 (HFD vs HFD–LFD, p = 0.015, Tmct) and IL-6 ($F_{(2,19)} = 7.052$, $p = 0.006$, ANOVA; HFD vs HFD–LFD, $p = 0.004$, Tmct) compared to HFD mice (Table 1), suggesting that potential anti-inflammatory changes accompanied the reduction in dietary fat content. Brain-derived neurotrophic factor (BDNF) has also been suggested as a link between diabetes and brain function (Fujinami et al., 2008). While we noted a trend of decreased BDNF levels in the hippocampus ($F_{(3,27)} = 2.253$, $p = 0.105$, ANOVA) and cortex ($F_{(3,27)} = 1.493$, $p = 0.239$, ANOVA) of HFD mice compared to all other groups, these differences did not reach significance (Table 1). Similarly, the neuropeptide glucagon-like peptide (GLP-1) also represents a potential link between diabetes and cognitive function, particularly in the background of a high fat diet

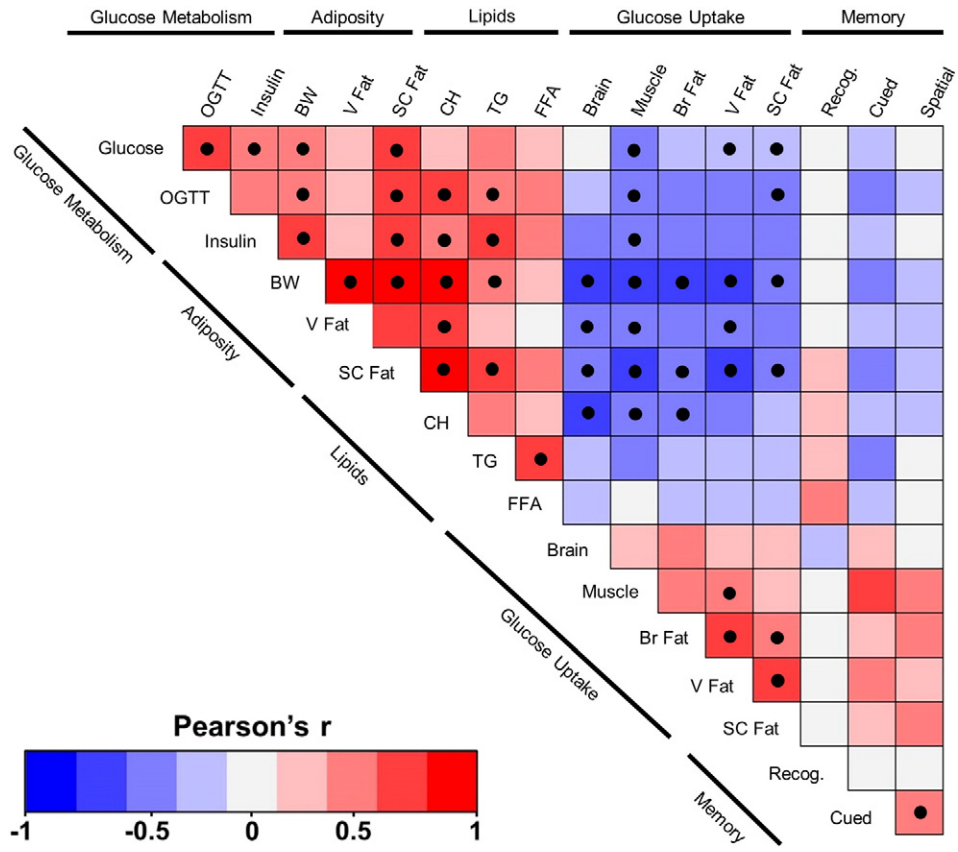

Fig. 3. Correlation Matrix of Physiological and Behavioral Measures. Measures of glucose metabolism, adiposity and dyslipidemia positively correlate with one another. Glucose uptake in various tissues positively correlates with one another, and negatively correlates with measures of glucose metabolism, plasma lipids, and degree of adiposity. The correlation matrix of physiological and behavioral measures is based on Pearson's linear correlation (Pearson's r rank correlation coefficients were computed using z-score transformed values). Black circles represent significant correlations after false discovery rate correction (Benjamini Hochberg method). Abbreviations (specific measure analyzed in parentheses): BW, body weight; Br Fat, brown fat; CH, cholesterol; Cued, cued memory (average time freezing in response to cue); FFA, free fatty acids; Nesting, nesting score; OGTT, oral glucose tolerance test (area under the curve); SC Fat, subcutaneous fat; Recog, object recognition memory (time spent exploring novel object); Spatial, spatial memory (cumulative distance to platform during 72 h memory probe); TG, triglycerides; V Fat, visceral fat.

Table 1
Physiologic and Metabolic Parameters in Experimental Mice.

	LFD	(*n*)	T1D	(*n*)	HFD	(*n*)	HFD–LFD	(*n*)
Physiological measures								
Body weight (g)	28.68 ± 1.204^{a}	14	24.44 ± 2.040^{b}	8	48.09 ± 4.300^{c}	13	28.33 ± 0.590^{a}	12
Visceral fat (g)	0.999 ± 0.643^{a}	14	0.346 ± 0.179^{b}	8	4.556 ± 4.036^{c}	13	0.988 ± 0.407^{a}	11
SC fat (g)	0.458 ± 0.186^{a}	14	0.288 ± 0.122^{b}	8	2.553 ± 1.245^{c}	13	0.601 ± 0.209^{a}	11
Plasma markers								
Glucose (mg/dl)	74.8 ± 15.76^{a}	15	408.6 ± 74.11^{b}	8	123.5 ± 19.15^{c}	14	102.7 ± 25.77^{d}	12
Insulin (ng/ml)	0.755 ± 0.433^{a}	9	*b.d.*	8	3.467 ± 3.719^{b}	9	0.360 ± 0.228^{c}	7
TC (mg/dl)	70.51 ± 6.06^{a}	9	119.5 ± 28.4^{b}	7	105.0 ± 14.34^{b}	8	67.03 ± 5.12^{a}	6
TG (mg/dl)	35.01 ± 3.94^{a}	9	48.61 ± 11.20^{b}	7	46.49 ± 11.71^{b}	8	37.18 ± 6.57^{a,b}	6
FFA (μM)	172.7 ± 38.32^{a}	7	253.3 ± 79.78^{b}	7	211.1 ± 79.78^{a,b}	8	175.6 ± 31.35^{a}	6
KB (μM/l)	98.85 ± 24.02^{a}	8	352.8 ± 225.6^{b}	7	182.8 ± 127.0^{a,b}	7	120.1 ± 35.15^{a}	5
GLP-1 (pg/ml)	8.724 ± 1.484^{a}	6	*n.d.*		5.888 ± 2.00^{a}	7	8.002 ± 2.822^{a}	5
BDNF (pg/mg protein)								
Hippocampus	129.8 ± 11.87^{a}	8	146.3 ± 42.49^{a}	9	91.03 ± 18.13^{a}	9	153.6 ± 32.38^{a}	6
Cortex	152.3 ± 19.72^{a}	8	203.7 ± 113.7^{a}	9	144.4 ± 20.43^{a}	9	163.0 ± 32.69^{a}	6
Plasma inflammatory markers								
IFN-γ (pg/ml)	1.986 ± 1.212^{a}	8	*n.d.*		1.912 ± 1.165^{a}	9	1.292 ± 0.225^{a}	6
IL-10 (pg/ml)	15.47 ± 6.28^{a}	8	*n.d.*		17.23 ± 5.77^{a}	9	16.73 ± 12.26^{a}	6
IL-12p70 (pg/ml)	42.84 ± 24.50^{a}	8	*n.d.*		44.70 ± 25.56^{a}	9	36.61 ± 25.80^{a}	6
IL-1b (pg/ml)	1.218 ± 1.318^{a}	8	*n.d.*		1.958 ± 2.206^{a}	9	0.865 ± 0.993^{a}	6
Cxcl1 (pg/ml)	135.9 ± 33.04^{a}	8	*n.d.*		236.2 ± 68.73^{b}	9	150.0 ± 26.18^{a}	6
TNFα (pg/ml)	2.829 ± 3.965^{a}	8	*n.d.*		3.052 ± 4.119^{a}	9	6.127 ± 4.178^{a}	6
IL-6 (pg/ml)	61.81 ± 28.30^{a}	8	*n.d.*		87.30 ± 43.03^{a}	9	21.03 ± 17.64^{b}	6

b.d., below detection; BDNF, brain derived neurotrophic factor; Cxcl1, chemokine (C-X-C motif) ligand 1; FFA, free fatty acids; GLP-1, glucagon-like peptide 1; HFD, high fat diet; IFN-γ, interferon-γ; IL-1b, interleukin-1β; IL-6, interleukin-6; IL-10, interleukin-10; IL-12p70, interleukin-12p70; KB, total ketone bodies; LFD, low fat diet; n.d., not determined; SC, subcutaneous; TC, total cholesterol; TG, triglycerides; TNFα, tumor necrosis factor-α. All parameters were measured at 15 months of age (following 6 months on diet). Plasma markers were measured following a 4 h fast. Means without common superscript differ significantly ($p < 0.05$, ANOVA followed by Tukey's multiple comparisons test).

(Lennox et al., 2014). We observed a decrease in plasma GLP-1 concentrations in HFD compared to both LFD and HFD–LFD mice (Table 1), however this difference did not reach significance ($F_{(3,15)} = 3.175$, $p = 0.071$, ANOVA).

3.2. Amelioration of Cognitive Impairments Following a Reduction in Dietary Fat Content

We next evaluated the effects of MetS and a reduction in dietary fat content on cognitive performance. Deficits in natural rodent behaviors such as nest building may reflect disrupted activities of daily living in people with cognitive impairment (Deacon, 2012). We observed that HFD mice constructed less complex nests than their LFD counterparts ($F_{(2,22)} = 10.25$, $p < 0.001$, ANOVA; HFD vs LFD, $p < 0.001$, Tmct), and normal nest building behavior was restored in HFD–LFD mice (Fig. 4A) (HFD vs HFD–LFD, $p = 0.02$, Tmct), although this behavior may instead be explained by adiposity and heat regulation. We next examined novel object recognition. Following two acclimation periods, mice were exposed to two identical objects and allowed to freely explore. The time spent exploring each of the two identical objects did not differ in any of the groups (Object 1 vs Object 2, LFD, $t_{(8)} = 0.416$, $p = 0.689$; HFD, $t_{(8)} = 1.156$, $p = 0.281$; HFD–LFD, $t_{(6)} = 1.192$, $p = 0.278$, paired t-test) (data not shown). Twenty-four hours later, mice were re-introduced to one of the previous familiar objects and a novel object. LFD and HFD–LFD mice showed a robust preference for the novel object ($t_{(8)} = 2.073$, $p = 0.01$; $t_{(6)} = 3.549$, $p = 0.004$, paired t-test, respectively), while HFD mice did not show a preference (Familiar object vs Novel object, $t_{(8)} = 0.791$, $p = 0.441$, paired t-test), suggesting impaired recognition memory (Fig. 4B).

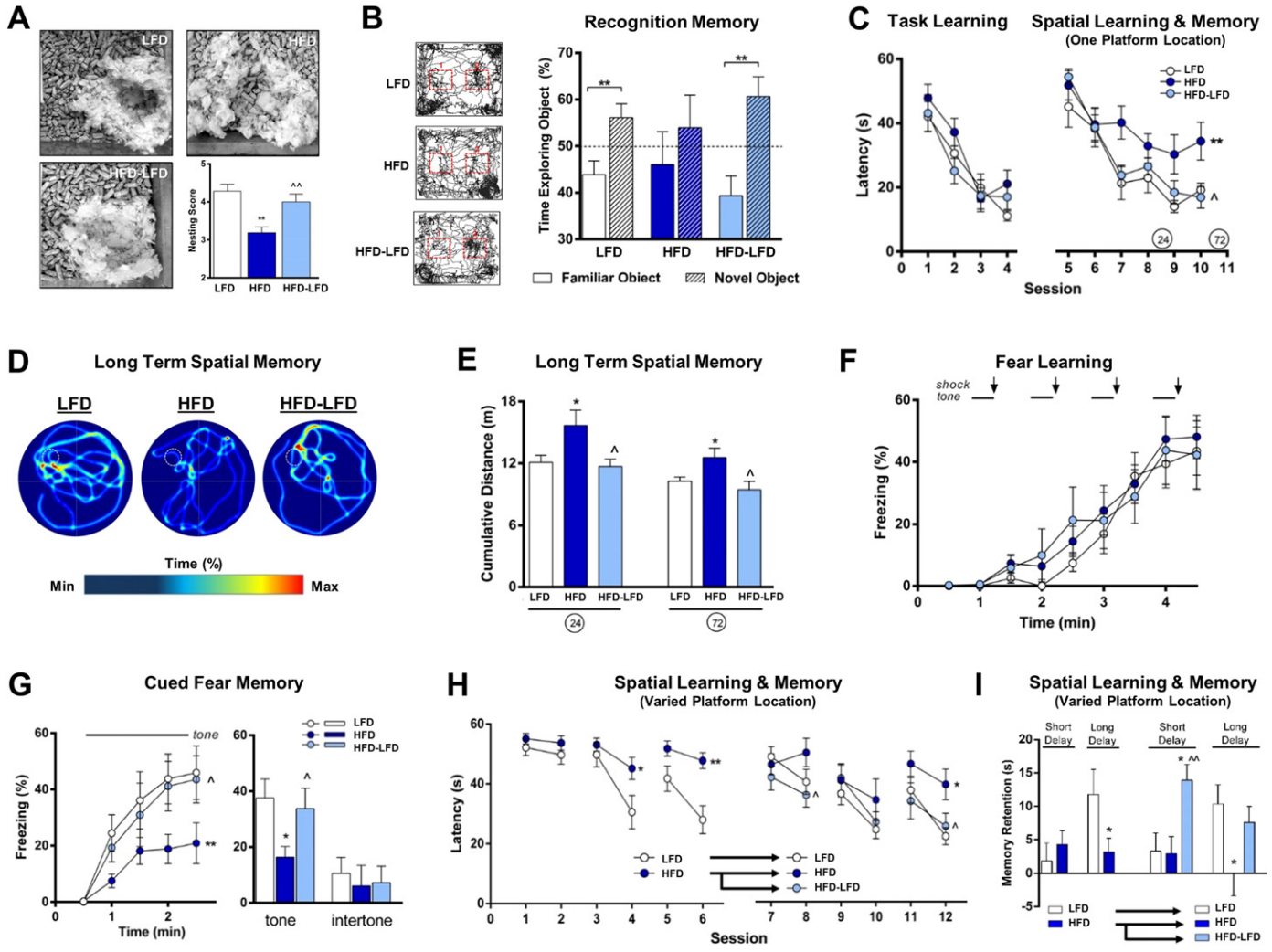

Fig. 4. MetS Results in Multiple Cognitive and Behavioral Impairments Which Are Rescued via a Reduction in Dietary Fat Content. (A) Nesting behavior is disrupted by HFD-induced MetS. Representative photos and mean scores of nests formed 48 h after nesting material is provided. (B) Recognition memory is impaired in HFD mice. HFD mice fail to show a preference for a novel object (box 2, striped bars) 24 h after exposure to a familiar object (box 1, open bars), as shown by video tracking (left panels) and time spent exploring each object. (C) MetS leads to deficiencies in spatial learning and memory. Latency to find a visible ("Task Learning", left) or hidden ("Spatial Learning and Memory", right) escape platform during the water maze. The timing (in hours) of tests of long-term memory retention (C–E) are noted by the circled numbers. (D–E) Long-term spatial memory is impaired in HFD mice. (D) Representative heat maps displaying swim patterns during a memory probe trial 72 h after the last training session. Platform location during hidden training is noted by the dashed white circle. (E) The accuracy of long-term spatial memory was measured by calculating the cumulative distance from the target platform location. Robust memory retention is reflected in more accurate search patterns, and thus lower cumulative distance values. (F) Fear learning is unaffected by MetS. Mice were conditioned to associate a cue (tone) with a mild foot shock. (G) Cued fear memory is impaired in HFD mice. Cued recall was assessed by measuring freezing in response to the tone 24 h after training. There were no differences in generalized fear, as indicated by freezing during the intertone period. (H) A short-term reduction in dietary fat content improves spatial learning and memory in HFD mice. Spatial learning and memory was tested using a modified water maze protocol in which the location of a hidden platform was varied daily (two sessions/day). Following the first round of testing (sessions 1–6), a subset of HFD mice were switched to a low fat diet for one month (HFD–LFD), and all mice were re-tested (sessions 7–12). (I) HFD–LFD mice show gains in memory retention. Memory retention was calculated as the decrease in latency between trials separated by a short (5 min) or long (3 h) delay. $^{*}p < 0.05$, $^{**}p < 0.01$ compared to LFD, $^{\wedge}p < 0.05$, $^{\wedge\wedge}p < 0.01$ compared to HFD, ANOVA, followed by Tukey's multiple comparison test. (*C*, *F*, *G*, *H* repeated measures ANOVA). (*A*–*G*, n = 7–9) (*H*–*I*, *n* = 9–11).

We then assessed spatial learning and memory in the water maze. Differences in vision, general task learning, anxiety or motor function could affect performance in the water maze. However, there were no group differences in the ability to locate a visible platform (Fig. 4C) ($F_{(2,22)} = 1.875$, $p = 0.178$, repeated measures ANOVA) (Supplemental Fig. 1A) ($F_{(2,27)} = 0.153$, $p = 0.860$, repeated measures ANOVA), suggesting that chronic HFD consumption does not affect task learning. There were also no differences in anxiety-like behavior in the open-field test (Supplemental Fig. 1B) ($F_{(2,22)} = 0.220$, $p = 0.804$, ANOVA), and despite concerns that obesity may affect motor ability, swim speeds did not significantly differ during the water maze (Supplemental Fig. 1C) ($F_{(2,22)} = 1.380$, $p = 0.273$, ANOVA). Conversely, HFD mice were diminished in their ability to locate a hidden escape platform, indicating impairments in spatial learning (Fig. 4C, right) ($F_{(2,22)} = 7.166$, $p = 0.004$, repeated measures ANOVA). Long-term spatial memory retention was assessed in probe trials in which the platform was removed and search patterns were analyzed. During both the 24 and 72 hour probe trials, HFD mice showed less accurate search patterns (Fig. 4D), as evidenced by an increase in the cumulative distance from the platform (Fig. 4E) (24 h, $F_{(2,22)} = 4.235$, $p = 0.028$, ANOVA; HFD vs LFD, $p = 0.043$, HFD vs HFD–LFD, $p = 0.044$, Tmct; 72 h, $F_{(2,22)} = 4.889$, $p = 0.017$, ANOVA; HFD vs LFD, $p = 0.033$, HFD vs HFD–LFD, $p = 0.025$, Tmct).

To test fear learning and cued fear memory, mice were trained to associate a cue (30 s tone) with a mild foot shock. All groups showed similar learning (Fig. 4F) ($F_{(2,22)} = 0.400$, $p = 0.675$, repeated measures ANOVA) and response to the shock (Supplemental Fig. 1D) ($F_{(2,22)} = 0.154$, $p = 0.852$, ANOVA) during the training day. However, HFD mice showed a decreased cued memory when reintroduced to the tone (Fig. 4G, tone) ($F_{(2,22)} = 3.955$, $p = 0.035$, repeated measures ANOVA; HFD vs LFD, $p = 0.036$, Tmct). This effect was not a result of differences in generalized fear (Fig. 4G, intertone) ($F_{(2,22)} = 0.06$, $p = 0.9417$, ANOVA), and the MetS-associated impairment in cued fear memory was rescued following the reduction in dietary fat content (Fig. 4G, tone) (HFD vs HFD–LFD, $p = 0.038$, Tmct).

To verify that the reduction in dietary fat content truly had a restorative effect on learning and memory, rather than simply being due to a threshold effect (i.e. five vs six months of high fat diet), we tested spatial learning and memory in an independent experiment before and after the intervention. Following five months of high fat diet, half of the HFD mice were randomly assigned to continue on high fat diet and half were administered the low fat diet intervention. During the initial test, HFD mice showed significant impairments in spatial learning and memory in a task that involved varied escape platform locations (Fig. 4H, left) (Sessions 3 and 4, $F_{(1,27)} = 3.940$, $p = 0.047$; Sessions 5 and 6, $F_{(1,27)} = 21.091$, $p < 0.001$, repeated measures ANOVA). Following the additional month, both LFD and HFD–LFD mice demonstrated superior performance compared to HFD mice (Fig. 4H–I, right) (Sessions 11–12, $F_{(2,26)} = 5.186$, $p = 0.013$, repeated measures ANOVA; HFD vs LFD, $p = 0.021$, HFD vs HFD–LFD, $p = 0.028$, Tmct). In particular, HFD mice struggled to retain memory of the platform location over the long delay (3 h) that separated the first and second daily testing sessions (Fig. 4I) (pre-intervention HFD vs LFD, $t_{(27)} = 2.202$, $p = 0.036$, *t*-test; post-intervention, $F_{(2,26)} = 3.367$, $p = 0.040$, ANOVA, HFD vs LFD, $p = 0.044$, Tmct). In contrast, HFD–LFD mice showed substantial improvements in memory retention, in particular during the short delay (5 min) (Fig. 4I, right) ($F_{(2,26)} = 5.605$, $p = 0.009$, ANOVA; HFD vs HFD–LFD, $p = 0.019$, LFD vs HFD–LFD, $p = 0.018$, Tmct).

We next asked if these cognitive deficits were universal to diabetes, or specific to the background of obesity, IR and MetS. To answer this question, we compared the cognitive profiles of HFD mice to diet- and age-matched siblings who were injected with streptozotocin (STZ), a model of type 1 diabetes (T1D). In contrast to T2D, where deficits in memory are noted even in early stages of the disease (Ruis et al., 2009), T1D patients generally show modest neurological impairments, and learning and memory are generally spared (Brands et al., 2005). Similarly, our results in an age- and diet-matched model of T1D showed very modest effects on learning and memory (Fig. 5). T1D mice showed profound peripheral metabolic impairments, including insulin deficiency, glucose intolerance, ketoacidosis and severe hyperglycemia (Table 1). However, their cognitive performance on tasks of novel object recognition (Fig. 5A) (Familiar object vs Novel object, LFD, $t_{(8)} = 2.073$, $p = 0.01$; T1D, $t_{(6)} = 3.232$, $p = 0.007$, paired *t*-test), spatial learning and memory (Fig. 5B) ($F_{(1,14)} = 0.754$, $p = 0.400$, repeated measures ANOVA), long term spatial memory (Fig. 5C–D) (24 h, $t_{(14)} = 1.490$, $p = 0.157$; 72 h, $t_{(14)} = 0.509$, $p = 0.619$, *t*-test), fear learning (Fig. 5E) ($F_{(1,14)} = 0.020$, $p = 0.889$, repeated measures ANOVA), and cued fear memory (Fig. 5F) ($F_{(1,14)} = 0.335$, $p = 0.572$, repeated measures ANOVA) was comparable to that of control mice. While T1D mice were slightly slower in general task learning, as seen in the visible portion of the water maze (Fig. 5B, left) ($F_{(1,14)} = 7.824$, $p = 0.015$, repeated measures ANOVA), they did not significantly differ from LFD controls by the end of training (Session 3, LFD vs T1D, $t_{(14)} = 0.679$, $p = 0.512$; Session 4, LFD vs T1D, $t_{(6)} = 1.769$, $p = 0.099$, *t*-test).

3.3. Cerebral Blood Volume Declines During MetS, Recovers Following a Reduction in Dietary Fat Content, and is Associated with Memory

To determine whether the cognitive impairments accompanying MetS are associated with alterations in cerebrovascular function, we measured cerebral blood volume (CBV) using optical microangiography (OMAG). OMAG allows for 3D volumetric quantification of blood-perfused vessels in the brain, at the capillary level, through an intact skull, *in vivo* and in real time (Jia et al., 2009). We focused our imaging on pial vessels that receive blood supply from the middle cerebral artery (MCA), as the MCA supplies several areas of the frontal, parietal and temporal cortices that play a role in the cognitive measures employed in this study, in particular components of the spatial learning and memory task involving varied platform locations (Bell et al., 2009; Curtis and D'Esposito, 2003; Haines, 2008; Postle, 2006; Smith and Jonides, 1999). Corresponding OMAG images of the same area of the brain were aligned for quantification of CBV before and after the intervention. HFD mice demonstrated reduced microvascular CBV in pial vessels within the analyzed cortical area (Fig. 6A–C) (CBV ≤ 10 μM vessel diameter, $F_{(3,31)} = 4.654$, $p = 0.008$, ANOVA; HFD (Image) vs LFD (Image), $p = 0.009$, Tmct). Re-imaging of the same vessel territories, in the same HFD mice, following the one month reduction in dietary fat content, revealed a significant increase in microvascular CBV, restoring CBV to similar levels as in controls (Fig. 6C) (HFD (Image) vs HFD–LFD (Re-image), ≤10 μM vessel diameter, $p = 0.022$; LFD (Re-Image) vs HFD–LFD (Re-image), ≤10 μM vessel diameter, $p = 0.787$, Tmct). Furthermore, spatial memory retention was positively correlated with microvascular CBV (Fig. 6D) ($r^2 = 0.822$, $p < 0.001$, Pearson). This phenomenon was specific to memory, as general task learning did not correlate with CBV (Supplemental Fig. 1E) ($r^2 = 0.001$, $p = 0.987$, Pearson).

To determine if the alterations in CBV were due to structural changes such as vessel rarefaction or neovascularization, we created polyurethane casts of the cerebral vasculature (Fig. 7A–C). Analysis of six distinct regions critical for performance in the spatial learning and memory water maze with varied platform locations (CA1, CA3, dentate gyrus, and the prelimbic, infralimbic, and cingulate cortex) did not reveal any differences in vessel volume or degree of vessel branching (Fig. 7D–I) (Volume, Hipp., $F_{(2,7)} = 0.991$, $p = 0.646$; Volume, PFC, $F_{(2,7)} = 0.620$, $p = 0.956$; Branching, Hipp., $F_{(2,7)} = 0.328$, $p = 0.895$; Branching, PFC, $F_{(2,7)} = 0.540$, $p = 0.841$, ANOVA). Taken together, these data suggest that the observed changes in CBV are likely functional, rather than structural, in origin.

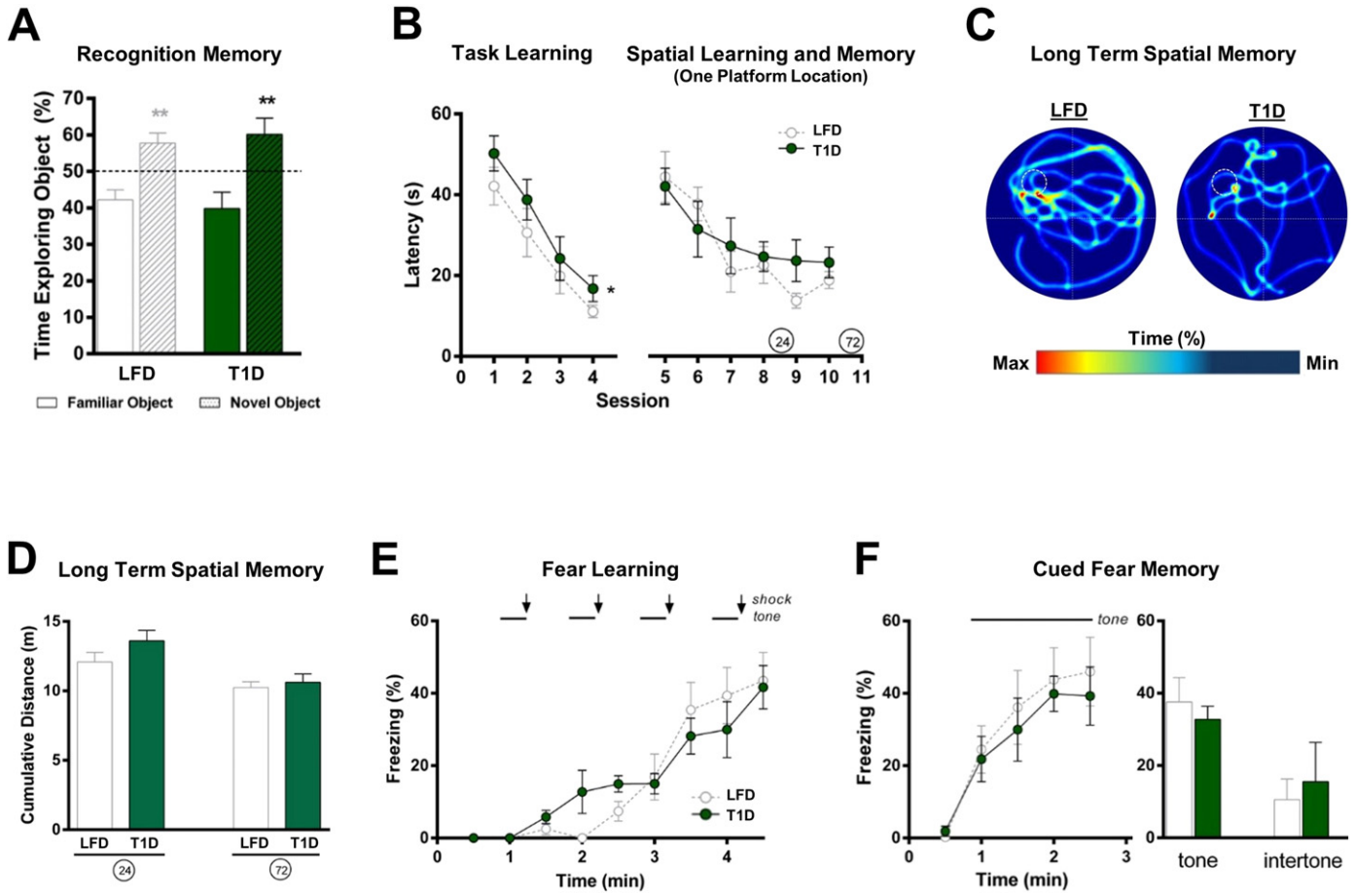

Fig. 5. Modest Cognitive Effects in a Model of Untreated Type 1 Diabetes. (A) Recognition memory is unaffected in mice with T1D (STZ treated). Twenty-four hours after exposure to a familiar object (open bars), mice were exposed to a novel object (striped bars). Control LFD mice and T1D mice both preferentially explore the novel object, suggesting memory of prior exposure to the familiar object. (B) T1D leads to slower task learning, but does not affect spatial learning and memory. Latency to find a visible or hidden escape platform during the water maze. The timing (in hours) of tests of long-term memory retention (C–D) are noted by the circled numbers. (C–D) Long-term spatial memory is unaffected in T1D mice. (C) Representative heat maps, displaying swim patterns during a probe trial given 72 h after the final water maze training session. The platform location during hidden training is noted by the dashed white circle. (D) The accuracy of long-term spatial memory was measured by calculating the cumulative distance from the target platform location. (E–F) (E) Fear learning and cued fear memory are unaffected by T1D. Mice were conditioned to associate a cue (tone) with a mild foot shock. (F) Cued memory was assessed by measuring freezing in response to the tone 24 h after conditioning. Generalized fear is indicated by freezing during the intertone period. $^{*}p < 0.05$, $^{**}p < 0.01$ compared to LFD, $\hat{}p < 0.05$, $\hat{}\hat{}p < 0.01$ compared to HFD, ANOVA, followed by Tukey's multiple comparison test. (*B*, *E*, *F* repeated measures ANOVA) ($n = 7$–9). LFD group data is reproduced from Fig. 2.

3.4. Infusion of LFD Plasma Mitigates Cognitive Impairments in HFD Mice and is Associated with a Distinct Metabolic Profile

Recent studies demonstrate remarkable neuro-restorative effects of young blood in aged mice (Villeda et al., 2014; Katsimpardi et al., 2014). We wished to test the hypothesis that plasma from LFD mice would have a beneficial effect on learning and memory, independent of age, in HFD mice. Over the course of ten days, plasma collected from age- and sex-matched sibling donors was repeatedly intravenously infused into HFD recipients (Fig. 8A). Compared to HFD mice who received plasma collected from other HFD mice, those receiving plasma from LFD mice performed significantly better on a spatial learning and memory task (Fig. 8B–C) (Day 7, $F_{(1,16)} = 4.996$, $p = 0.040$, repeated measures ANOVA; Day 7 Mean Latency, $t_{(16)} = 2.173$, $p = 0.045$; Day 10, $F_{(1,16)} = 10.153$, $p = 0.006$, repeated measures ANOVA; Day 10 Mean Latency, $t_{(16)} = 2.848$, $p = 0.012$, *t*-test). This cognitive improvement occurred independently of changes in body weight ($t_{(16)} = 0.153$, $p = 0.880$, *t*-test), plasma glucose ($t_{(16)} = 0.511$, $p = 0.616$, *t*-test), or motor function ($t_{(16)} = 0.131$, $p = 0.898$, *t*-test) (Supplemental Fig. 2A–C).

To evaluate potential metabolic pathways which could underlie the observed improvements in learning and memory in HFD mice following exposure to LFD plasma, we used an untargeted metabolomics approach. Plasma collected from HFD recipient mice following completion of their final cognitive test was analyzed using high-performance liquid chromatography in combination with quadrupole time-of-flight mass spectrometry. We identified 243 metabolites (Supplemental Table 1), of which 45 differed significantly in abundance between HFD mice receiving LFD versus HFD plasma (Fig. 8D). The profile was dominated by alterations in amino acid (AA) and lipid metabolism. HFD mice receiving LFD plasma showed lower concentrations of several AAs and their metabolic byproducts, including methionine, proline, homoserine and lysine. HFD mice receiving LFD plasma also showed higher concentrations of numerous glycerolipids (GL), in particular phosphatidylcholines (PC) and phosphatidylethanolamines (PE) (Fig. 8D).

To generate a global metabolome view, and to examine whether any particular metabolic 'hubs' were affected, we performed a pathway impact analysis using a relative-betweenness centrality measure. The impact analysis confirmed that the primary alterations were in AA and glycerophospholipid (GPL) metabolism (Fig. 8E). Specifically, the pathways most impacted by plasma infusion were GPL metabolism, arachidonic acid metabolism, GL metabolism, cysteine and methionine metabolism, lysine degradation, and glycosylphosphatidylinositol (GPI) anchor biosynthesis (Fig. 8E). We then used a random forest (RF) supervised class prediction model to determine the capacity of the metabolome to accurately classify mice into their respective groups,

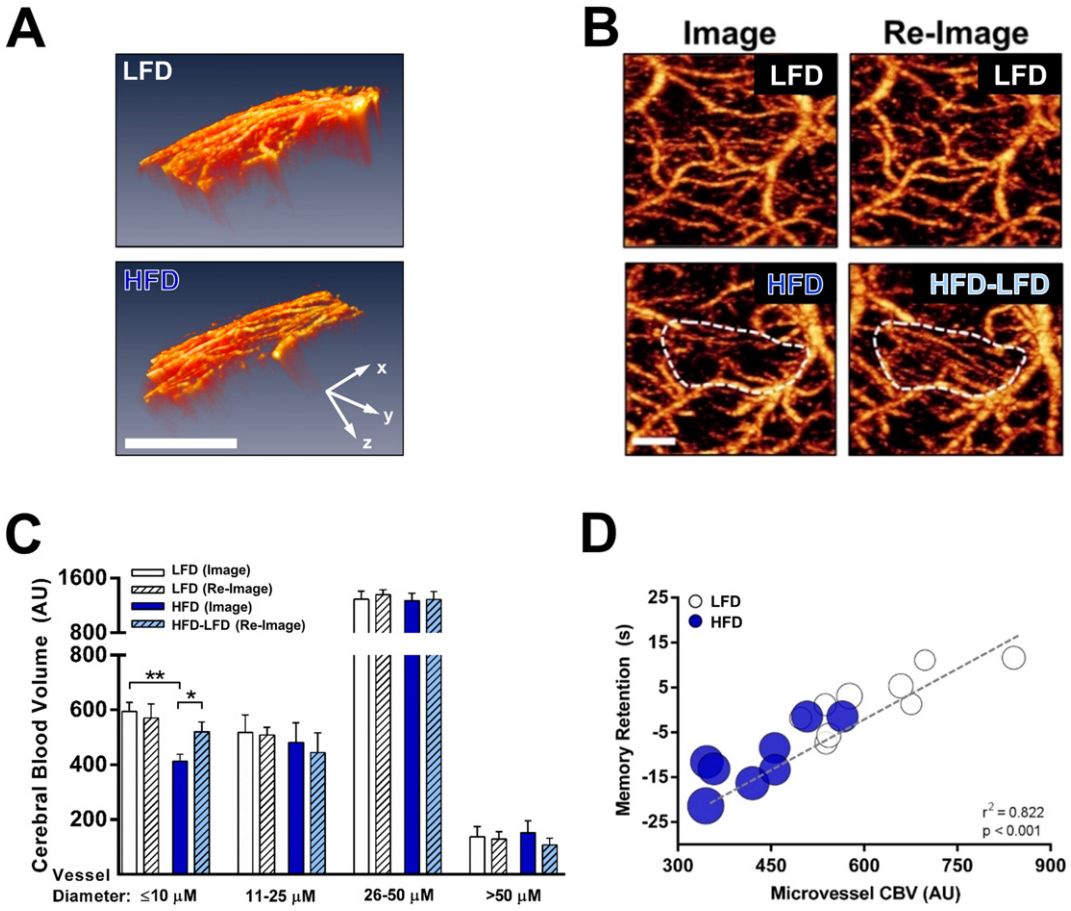

Fig. 6. Cerebral Blood Volume Declines During MetS, Recovers Following a Reduction in Dietary Fat Content, and is Associated with Memory. (A) Representative 3D images of cerebral blood volume (CBV) in vessels supplied by the middle cerebral artery. CBV was measured through an intact skull using optical micro-angiography. Scale bar 1 mM. (B–C) HFD-induced MetS is associated with decreased microvascular CBV, and a reduction in dietary fat content restores CBV to a similar level as controls. (B) Representative 2D-compressed images of CBV before and after a reduction in dietary fat content. The top row shows an area of the cortical surface of a LFD mouse imaged after five months, and re-imaged after six months, of low fat diet. The bottom row shows a mouse fed a high fat diet for 5 months (HFD), and then re-imaged following a one month reduction in dietary fat content (HFD–LFD). Microvascular CBV increased in HFD–LFD mice, as highlighted by the dotted white line. Scale bar 100 μM. (C) CBV within vessels of various diameters before ("Image") and after ("Re-Image") the low fat diet intervention. (D) Microvascular CBV positively correlates with cognitive performance in a spatial memory task. Memory retention is defined as the change in latency to find the platform over a three hour period. Body weight is represented by symbol diameter. $^{*}p < 0.05$, $^{**}p < 0.01$, ANOVA, followed by Tukey's multiple comparison test. (*D*, two-tailed Pearson correlation) (*C–D*, $n = 8–9$).

and to identify the specific metabolites most important to this prediction. The RF predictor correctly stratified 8/9 HFD receiving HFD plasma and 9/9 HFD receiving LFD plasma mice, for a cumulative predictive accuracy of 94%. The RF analysis defined the top 20 metabolites that together constitute the best predictors of group status, including numerous GPLs with high predictive accuracy (Fig. 8F). Together, these data indicate that repeated infusion of LFD plasma into HFD mice results in cognitive improvement characterized by a distinct plasma metabolic profile.

4. Discussion

In the present study, we highlight the malleable nature of MetS-associated cognitive dysfunction using a mouse model of chronic high fat diet (HFD) consumption. We show that a short-term reduction in dietary fat content results in improvements in peripheral metabolism, increased cerebral blood volume (CBV), and substantial gains in cognitive function in HFD mice. Additionally, we show that the administration of plasma collected from low fat diet (LFD) mice improves cognitive function in HFD mice, suggesting the involvement of systemic factors.

Increased adiposity in middle age drives risk of dementia in later life (Luchsinger and Gustafson, 2009) and the prevalence of cognitive impairment is higher in women (Hebert et al., 2013). Therefore, we induced obesity, IR and MetS in "middle aged" female mice (9 months old) via chronic administration of a high fat diet and assessed metabolic, vascular and cognitive effects during old age (14–15 months of age). HFD mice demonstrated several hallmarks of MetS commonly seen in human patients, including hyperglycemia, hyperinsulinemia, impaired glucose tolerance, decreased insulin sensitivity, dyslipidemia and reductions in peripheral and brain glucose uptake. Importantly, HFD mice showed cognitive deficits in multiple areas, including object recognition, cued memory, and spatial learning and memory. These results confirm multiple studies which have demonstrated behavioral and neurobiological impairments using genetic and diet-induced rodent models of obesity and T2D (Gault et al., 2010; Li et al., 2002; Stranahan et al., 2008a, 2008b; Winocur et al., 2005).

Interestingly, these cognitive impairments were not observed in a model of T1D, as mice with STZ-induced diabetes performed these tasks at levels similar to age-matched controls. While several studies have demonstrated cognitive dysfunction in rodent models of T1D (Biessels et al., 1996; Ramanathan et al., 1998; Alvarez et al., 2009; Rajashree et al., 2011), our data is consistent with human studies where learning and memory are generally spared in T1D patients (Brands et al., 2005), while multiple memory deficits are noted even in the early stages of T2D (Ruis et al., 2009). It should be noted, however, that differential metabolic effects have been observed depending on the mouse strain and caloric source, i.e. high fat vs high-sucrose diets (Surwit et al., 1995; West et al., 1995). Thus, while similar cognitive

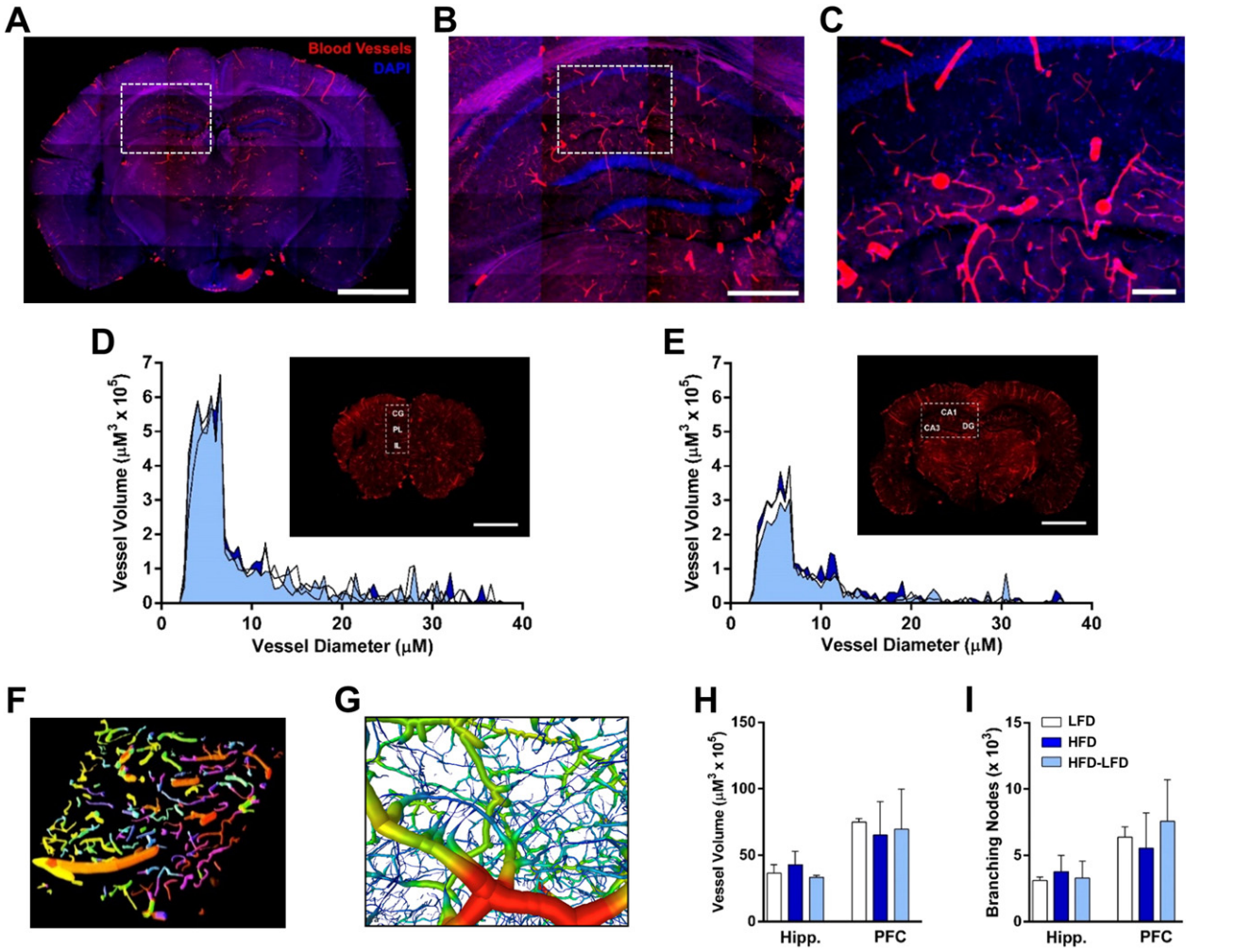

Fig. 7. Cerebral Vessel Density is Unaltered in HFD and HFD–LFD Mice. (A–C) Representative images of vascular casting within the brain. (A) Image montage of a full coronal brain section, taken at 4× magnification. Red = vessels (casting agent). Blue = nuclei (DAPI). Scale bar, 2 mm. (B) Image montage of the hippocampus, taken at 10×. Scale bar, 500 μm. (C) Representative image of the CA1 region of the hippocampus, taken at 10×. Scale bar, 100 μm. (D–E) Blood vessel volume is unaffected by MetS. The volume of blood vessels within specific regions of the (D) prefrontal cortex (cingulate (CG), prelimbic (PL) and infralimbic (IL)) and (E) hippocampus (CA1, CA3, and dentate gyrus (DG)). Insets show representative coronal brain sections that have been perfused with a fluorescent casting agent. Red = vessels (casting agent). Scale bar = 2 mM. (F–G) Representative images from a 3D analysis of vessel diameter and volume. (F) Physically contiguous vessels were identified and vessel diameter and volume were calculated using 4Quant software (colors correspond to vessel region and diameter). (G) Vessel diameter and volume were calculated in a 3D stack using Amira software (color corresponds to vessel diameter). (H–I) (H) Total vessel volume and (I) number of vessel branching points within 3D areas of the hippocampus and prefrontal cortex. (*H*, *I* ANOVA, followed by Tukey's multiple comparison test.) ($n = 3$–4).

impairments in rodents can be brought on by increased caloric intake in the form of either simple carbohydrates or saturated fats (Kanoski and Davidson, 2011), it is important to point out that the metabolic and cognitive effects observed in this study may still be specific to a high fat diet. Additionally, as we employed only high-fat fed female mice of advanced age, the extent to which these data extend across sex, age and degree of metabolic dysfunction is unclear, and further studies are needed to elucidate these issues.

In order to examine the effects of weight loss and improvements in metabolism on cognitive function, we subjected HFD mice to a brief, but intensive reduction in dietary fat and caloric intake. This one month low-fat diet intervention improved nearly every measure of peripheral metabolism and led to a complete restoration of the cognitive deficits associated with MetS. The intervention employed in this study would be considered extreme by human standards, and although translation is difficult given the differences in lifespan between mice and humans, perhaps the most appropriate comparison is the extensive weight loss observed in obese patients following bariatric surgery. There is evidence of rapid improvement in memory among bariatric surgery patients (Gunstad et al., 2011), and together with other weight loss studies reporting improvement in various cognitive domains (Siervo et al., 2011), the data presented here suggest that the cognitive dysfunction associated with MetS is at least partially reversible. Unfortunately, a very small percentage of patients with T2D makes the significant lifestyle changes necessary to send the disease into remission (Karter et al., 2014). However, recent work suggests that time restricted feeding (Chaix et al., 2014) and intermittent fasting (Brandhorst et al., 2015) may provide similar metabolic and/or cognitive benefits, and thus may represent more easily adoptable behavioral interventions for obese individuals and patients with MetS or T2D.

Memory impairment as a result of neurodegeneration, as in cases of Alzheimer's disease (AD) and Vascular Dementia (VsD) is believed to be largely irreversible once it occurs. In general, the cognitive deficiencies associated with MetS and T2D appear to occur early, perhaps in concert with the obesity and IR which typically occur prior to overt diabetes (Kim and Feldman, 2015; Ruis et al., 2009; Sellbom and Gunstad, 2012). The model employed here reflects these early stages of T2D in humans, and it is probable that there becomes a point at which the cognitive dysfunction associated with T2D becomes irreversible. For example, there is evidence of decreased brain volume (Espeland et al., 2013)

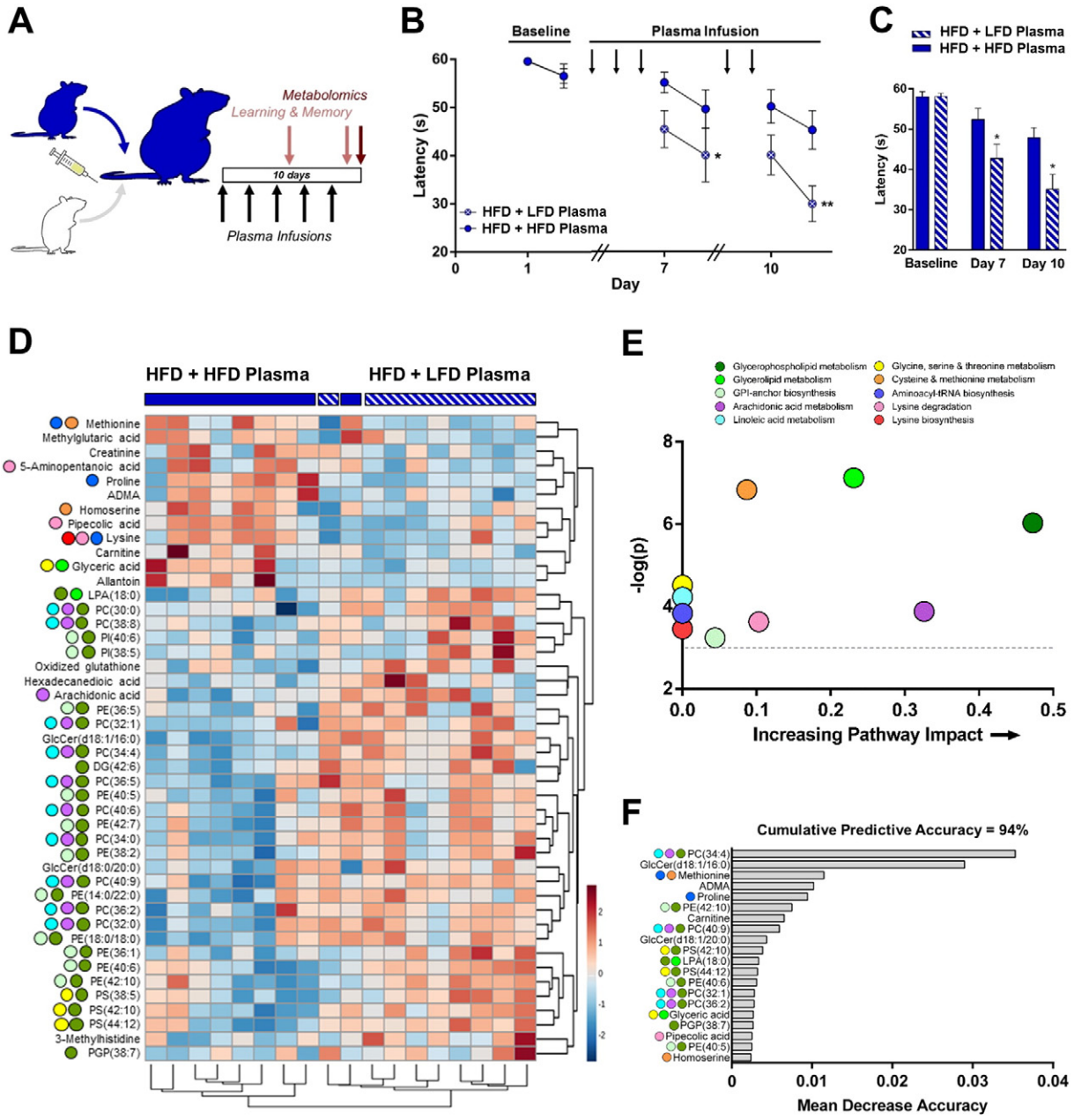

Fig. 8. Infusion of LFD Plasma Improves Memory in HFD Mice and is Associated with a Distinct Metabolic Profile. (A) Experimental design. Plasma was collected from age-matched LFD (LFD plasma) or HFD mice (HFD plasma). HFD recipients were intravenously injected with 100 μl of pooled plasma every other day for 10 days. Twenty-four hours following the final infusion, plasma was collected from recipient mice for an untargeted metabolomics analysis. (B–C) Infusion of LFD plasma is sufficient to improve cognitive function in HFD mice. HFD mice injected with plasma collected from age-matched LFD control mice located a hidden platform faster than HFD mice injected with plasma collected from other HFD mice. Latency to platform within (B) individual testing sessions and (C) daily averages (mean of two testing sessions). (D) Two-way hierarchical clustering of the 45 plasma metabolites that significantly differ ($p < 0.05$) between HFD recipient mice infused with LFD or HFD plasma. Color in the heat map reflects the relative metabolite abundance level, with red being higher, and blue lower, than the mean value. Colored circles denote the metabolic pathway(s) in which each metabolite plays a role. (E) A global view of the metabolome was created using a pathway impact analysis. The metabolome view reflects increasing pathway impact according to the betweenness centrality measure, which reflects key nodes in pathways that have been significantly altered by infusion of 'healthy' plasma. Only pathways with a significance of $p < 0.05$ are shown (above the dotted gray line). (F) Random forest (RF) prediction using global metabolomic expression profiles. Mean decrease accuracy represents the percent decrease in accuracy of the RF analysis when the algorithm is performed in the absence of the indicated biomarker. The RF plot shows that the identified metabolites stratify the recipient mice according to donor plasma status with a cumulative predictive accuracy of 94%. (*B*, $^{*}p < 0.05$, $^{**}p < 0.01$ compared to HFD + HFD plasma, repeated measures ANOVA). (*C*, $^{*}p < 0.05$, *t*-test). ($n = 9$). (Abbreviations: ADMA, Asymmetric dimethylarginine; DG, Diacylglycerol; GlcCer, Glucosylceramide; LPA, Lysophosphatidic acid; PC, Phosphatidylcholine; PE, Phosphatidylethanolamine; PG, Phosphatidylglycerol; PGP, phosphatidylglycerolphosphate; PI, Phosphatidylinositol; PS, Phosphatidylserine).

and exacerbation of cerebrovascular and Alzheimer's disease (AD) pathology in diabetic humans (Peila et al., 2002; Ahtiluoto et al., 2010; Sonnen et al., 2009) and rodents (Park, 2011). In these cases, it is less likely that a simple lifestyle intervention would significantly improve neurological function. Given the resistance of T2D to therapy in its late stages, it becomes critical for future studies to determine if and when this "point of no return" occurs, and intervene with medical and public health initiatives focused on early stages of the disease.

Some evidence suggests that inflammation may serve as the causative link between diabetes, cerebrovascular function and cognitive

dysfunction (Chung et al., 2015; Novak et al., 2011). While generally increased in HFD mice, a number of plasma cytokines – including IL-12p70, IL1βF, TNFα, and IFNγ – did not significantly differ from the LFD or HFD–LFD groups. We did, however, observed a pronounced change in CXCL1, a neutrophil chemoattractant with pro-angiogenic properties (Miyake et al., 2013). Circulating CXCL1 levels were increased in HFD mice, but similar to LFD levels in HFD–LFD mice. CXCL1 crosses the blood brain barrier (BBB) (Pan and Kastin, 2001), is elevated in patients with T2D (Sajadi et al., 2013) as well as those with AD (Zhang et al., 2013), and thus represents a potential link between diabetes, inflammation, cerebrovascular function and cognition. Along these lines, neuroprotective molecules such as BDNF, which is decreased in the serum of T2D patients (Fujinami et al., 2008), have also been suggested as a link between diabetes and brain function. Similarly, the neuropeptide GLP-1 and its long-lasting analogs have received much attention in recent years due to their potential to treat T2D (Kern et al., 2001). GLP-1 readily crosses the BBB and its receptors are expressed in multiple brain regions (Hamilton and Hölscher, 2009). Furthermore, treatment with GLP-1 in rodent models of several neurological disorders, including high fat fed mice (Lennox et al., 2014), has been shown to stimulate neurogenesis (Rampersaud et al., 2012), improve long-term potentiation (Gault and Hölscher, 2008), and improve cognitive function (Lennox et al., 2014; Rachmany et al., 2013; Solmaz et al., 2015). While we observed lower plasma GLP-1 concentrations in HFD mice compared to both LFD and HFD–LFD mice, this difference did not reach statistical significance. It should be noted, however, that the multiple plasma markers described above, in which a trend was observed but statistical significance was not reached, are likely due to study limitations in power. Thus, the potential cognitive effects of these various inflammatory, neurotrophic and metabolically active factors still represent plausible biological mechanisms by which both weight loss and infusion of 'healthy' plasma may exert beneficial effects, particularly if acting in concert or in parallel.

Another potential modifiable link between diet-induced metabolic and cognitive dysfunction is the regulation of cerebral blood flow (CBF) (Barnes and Joyner, 2012). In some studies, individuals with T2D show lower CBF (Novak et al., 2006) and a reduced ability to maintain adequate and stable CBF compared to controls (Kim et al., 2008). At normal physiological concentrations in the periphery, insulin acts as a vasomodulator by stimulating microvascular perfusion (Lambadiari et al., 2015). In patients with T2D, administration of intranasal insulin results in enhanced cognition which may be mediated via vasoreactive effects (Novak et al., 2014). Interestingly, evidence from coronary vessels suggests that the mechanism by which insulin exerts its vasodilatory effects differs depending on vessel size (Oltman et al., 2000). Our results show that improvements in CBV, a measure reflective of vascular perfusion, following the reduction in dietary fat content were specific to microvessels. The microvascular response to insulin appears to rely heavily on capillary recruitment (Shim et al., 2014; Dawson et al., 2002; Vincent et al., 2002). In skeletal muscle and adipose tissue, the microvasculature is particularly sensitive to insulin, and this sensitivity is impaired by obesity and IR (Belcik et al., 2015). Our data suggest that a similar phenomenon may occur in the brain, with specific reductions in microvascular CBV during MetS and a subsequent increase following restoration of insulin sensitivity.

Alternative to impairments in insulin-mediated vasoreactivity, the observed decrease in microvascular CBV during MetS could be explained by structural abnormalities. Decreases in vessel density due to microvascular rarefaction occur in several chronic diseases, including obesity (Pasarica et al., 2009). However, both increased cerebral angiogenesis (Ergul et al., 2014) and decreased cerebral vessel density have been reported in diabetic rodents (Beauquis et al., 2010). While we observed regional differences in capillary density, as shown by others (Cavaglia et al., 2001), we did not observe any changes in vessel density, of any diameter, between LFD, HFD, and HFD–LFD mice.

As vascular function represents a critical link between diabetes and cognition, it is plausible that circulating factors could affect brain function. Experiments involving shared circulatory systems have played a crucial role in the study of obesity and T2D (Coleman, 2010), and a series of studies have shown that young blood has numerous rejuvenative properties in aging mice (Villeda et al., 2014; Ruckh et al., 2012; Salpeter et al., 2013; Loffredo et al., 2013; Katsimpardi et al., 2014). However, these recent experiments all highlight a dichotomy between the young and old. To the best of our knowledge, our study represents the first evidence that plasma infusion also holds promise in the age-independent context of MetS. Here, infusion of plasma collected from lean, non-diabetic LFD donors was sufficient to improve cognitive function in HFD mice, and this improvement occurred in the face of concurrent obesity and continued consumption of a high fat diet. These data suggest that administration of plasma, or of specific factors found within, may represent a potential strategy for the treatment of the cognitive complications of diabetes.

It is unlikely that the cognitive gains observed following plasma infusion are solely due to one factor, as recent contradictory findings in aging studies indicate (Loffredo et al., 2013; Egerman et al., 2015). Additionally, dilution and temporal factors likely reduce the impact of any one individual factor; for example, HFD mice received 100 μl infusions but have >2.5 ml total blood volume and the analysis occurred 24 h after the final infusion. In this regard, while our untargeted metabolomics analysis revealed 45 significantly altered metabolites, the effect size of each individual factor was small (fold change for 99% of metabolites was <2.0). Still, two main patterns of note were revealed in HFD mice infused with 'healthy' LFD plasma: lower concentrations of multiple AAs and their byproducts, and higher concentrations of numerous GPLs. Elevated levels of branched chain (bc) AAs are associated with obesity and IR, and are predictive of future development of T2D (Newgard et al., 2009; Wang et al., 2011). However, we did not observe significant changes in bc AAs, likely because both plasma recipient groups still had MetS. Instead, our analysis revealed alterations in several AAs that more closely resemble the metabolic changes that accompany aging (Houtkooper et al., 2011). The analysis also highlighted alterations in various classes of GPLs, particularly PEs and PCs. While it is unclear how elevated plasma concentrations of PEs and PCs affect cognitive function, they are present in relatively high amounts in neural membranes where they play metabolic, structural and functional roles (Farooqui et al., 2000). Moreover, lower levels of brain GPLs have been associated with neurodegenerative disease (Wood et al., 2015). Additionally, a common second messenger produced from PEs and PCs is arachidonic acid, which was also significantly elevated in HFD mice receiving infusions of LFD plasma. Arachidonic acid is a common precursor to several vasoactive eicosanoids which represent an intriguing biological link between IR, microvascular function and cognition (Iliff et al., 2009; Shim et al., 2014). Also of interest is asymmetric dimethylarginine (ADMA), a methylated form of L-arginine, which was present in significantly lower concentrations in HFD mice receiving infusions of LFD plasma. ADMA has been proposed as a potential link between vascular disease and dementia, as it is found in higher concentrations in T2D individuals (Abbasi et al., 2001) and inhibits nitric oxide synthesis and vasodilation (Asif et al., 2013).

Another limitation of the current study is that it remains unknown whether the observed cognitive benefits associated with plasma infusion are a result of direct modulation of neuronal function, secondary to peripheral metabolic changes, or a more complicated cascade of events involving both. Despite our observations that body weight, blood glucose and swim speed were unchanged by plasma infusion, there remain numerous indirect mechanisms through which the plasma infusions could modulate brain function, including effects on general metabolism, stress response, appetite, gut hormones, immune mediators, and vascular

function. Thus, future studies aimed at elucidating the precise biological mechanisms underlying the cognitive benefits associated with weight loss and improvements in metabolism, as well as those associated with plasma infusion, are critical.

In summary, this work highlights the malleable nature of diet-induced cognitive dysfunction. We hope that this study will spur future research and inspire individual lifestyle changes aimed at preventing or ameliorating the cognitive decline associated with obesity, IR and T2D.

Supplementary data to this article can be found online at http://dx.doi.org/10.1016/j.ebiom.2015.12.008.

Funding

L.A.J. was supported by NIEHS grant T32-ES07060, NIH grant T32-HL094294, NSF grant SMA-1408653, the Collins Medical Trust, an OHSU Tartar Award, the Oregon Tax Check-off Program for Alzheimer's Research administered by the Layton Aging & Alzheimer's Disease Center at OHSU, and the OHSU development account of J.R. K.L.Z. was supported by NIH F32NS082017. N.J.A. was supported by NIH R21AG043857. D.G.Z. was supported by NIDA T32DA007262. J.F.S. was supported by NIH grant S10RR027878 and the OSU Mass Spectrometry Core Facility of the Environmental Health Sciences Center grant P30ES000210. The funding sources had no role in the writing of the manuscript or the decision to submit it for publication. The contents of the manuscript are solely the responsibility of the authors and do not necessarily represent the official views of the funding agencies.

Conflicts of Interest

There are no conflicts of interest to report.

Acknowledgments

The authors would like to thank Tunde Akinyeke, Erin Bidiman, Alicia Callejo-Black, Massarra Eiwaz, Colton Erickson, Anna-Maria Hartner, Jackie Lanz, Collin McCormack, Wendy McGinnis, Dominic Siler, Marco Stampanoni, Blair Stewart, Eduardo Tellez, Eileen Torres and Hime Worku for their invaluable assistance.

References

Abbasi, F., Asagmi, T., Cooke, J.P., Lamendola, C., McLaughlin, T., Reaven, G.M., Stuehlinger, M., Tsao, P.S., 2001. Plasma concentrations of asymmetric dimethylarginine are increased in patients with type 2 diabetes mellitus. Am. J. Cardiol. 88, 1201–1203.

Ahtiluoto, S., Polvikoski, T., Peltonen, M., Solomon, A., Tuomilehto, J., Winblad, B., Sulkava, R., Kivipelto, M., 2010. Diabetes, Alzheimer disease, and vascular dementia. A population-based neuropathologic study. Neurology 75, 1195–1202.

Alvarez, E.O., Beauquis, J., Revsin, Y., Banzan, A.M., Roig, P., De Nicola, A.F., et al., 2009. Cognitive dysfunction and hippocampal changes in experimental type 1 diabetes. Behav. Brain Res. 198 (1), 224–230.

Asif, M., Soiza, R.L., McEvoy, M., Mangoni, A.A., 2013. Asymmetric dimethylarginine: a possible link between vascular disease and dementia. Curr. Alzheimer Res. 10 (4), 347–356 (May 1).

Baker, L.D., Cross, D.J., Minoshima, S., Belongia, D., Watson, G.S., Craft, S., 2011. Insulin resistance and Alzheimer-like reductions in regional cerebral glucose metabolism for cognitively normal adults with prediabetes or early type 2 diabetes. Arch. Neurol. 68, 51–57.

Barnes, J.N., Joyner, M.J., 2012. Sugar highs and lows: the impact of diet on cognitive function. J. Physiol. 590 (Pt 12), 2831.

Beauquis, J., Homo-Delarche, F., Giroix, M.H., Ehses, J., Coulaud, J., Roig, P., Portha, B., De Nicola, A.F., Saravia, F., 2010. Hippocampal neurovascular and hypothalamic–pituitary–adrenal axis alterations in spontaneously type 2 diabetic GK rats. Exp. Neurol. 222 (1), 125–134.

Belcik, J.T., Davidson, B.P., Foster, T., Qi, Y., Zhao, Y., Peters, D., Lindner, J.R., 2015. Contrast-enhanced ultrasound assessment of impaired adipose tissue and muscle perfusion in insulin-resistant mice. Circ. Cardiovasc. Imaging 4 (pii: e002684).

Bell, R., Severson III, M.A., Armonda, R.A., 2009. Neurovascular anatomy: a practical guide. Neurosurg. Clin. N. Am. 20 (3), 265–278. http://dx.doi.org/10.1016/j.nec.2009.04.012 (Jul).

Biessels, G.J., Kamal, A., Ramakers, G.M., Urban, I.J., Spruijt, B.M., Erkelens, D.W., Gispen, W.H., 1996. Place learning and hippocampal synaptic plasticity in streptozotocin-induced diabetic rats. Diabetes 45, 1259–1266.

Bigornia, S.J., Mott, M.M., Hess, D.T., Apovian, C.M., McDonnell, M.E., Duess, M.A., Kluge, M.A., Fiscale, A.J., Vita, J.A., Gokce, N., 2010. Long-term successful weight loss improves vascular endothelial function in severely obese individuals. Obesity (Silver Spring) 4, 754–759.

Blumenthal, J.A., Babyak, M.A., Sherwood, A., Craighead, L., Lin, P.-H., Johnson, J., et al., 2010. Effects of the dietary approaches to stop hypertension diet alone and in combination with exercise and caloric restriction on insulin sensitivity and lipids. Hypertension 55, 1199–1205.

Brandhorst, S., Choi, I.Y., Wei, M., Cheng, C.W., Sedrakyan, S., Navarrete, G., Dubeau, L., Yap, L.P., Park, R., Vinciguerra, M., Di Biase, S., et al., 2015. A periodic diet that mimics fasting promotes multi-system regeneration, enhanced cognitive performance, and healthspan. Cell Metab. 1, 86–99.

Brands, A.M., Biessels, G.J., de Haan, E.H., Kappelle, L.J., Kessels, R.P., 2005. The effects of type 1 diabetes on cognitive performance: a meta-analysis. Diabetes Care 3, 726–735.

Brinkworth, G.D., Buckley, J.D., Noakes, M., Clifton, P.M., Wilson, C.J., 2009. Long-term effects of a very low-carbohydrate diet and a low-fat diet on mood and cognitive function. Arch. Intern. Med. 169, 1873–1880.

Bruce-Keller, A.J., Keller, J.N., Morrison, C.D., 2009. Obesity and vulnerability of the CNS. Biochim. Biophys. Acta 1792, 395–400.

Cavaglia, M., Dombrowski, S.M., Drazba, J., Vasanji, A., Bokesch, P.M., Janigro, D., 2001. Regional variation in brain capillary density and vascular response to ischemia. Brain Res. 910 (1–2), 81–93 (Aug 10).

Chaix, A., Zarrinpar, A., Miu, P., Panda, S., 2014. Time-restricted feeding is a preventative and therapeutic intervention against diverse nutritional challenges. Cell Metab. 6, 991–1005.

Cheng, G., Huang, C., Deng, H., Wang, H., 2012. Diabetes as a risk factor for dementia and mild cognitive impairment: a meta-analysis of longitudinal studies. Intern. Med. J. 5, 484–491.

Chung, C.C., Pimentel, D., Jor'dan, A.J., Hao, Y., Milberg, W., Novak, V., 2015. Inflammation-associated declines in cerebral vasoreactivity and cognition in type 2 diabetes. Neurology 85 (5), 450–458. http://dx.doi.org/10.1212/WNL.0000000000001820 (Aug 4).

Coleman, D.L., 2010. A historical perspective on leptin. Nat. Med. 10, 1097–1099.

Curtis, C.E., D'Esposito, M., 2003. Persistent activity in the prefrontal cortex during working memory. Trends Cogn. Sci. 7 (9), 415–423 (Sep.).

Dawson, D., Vincent, M.A., Barrett, E.J., Kaul, S., Clark, A., Leong-Poi, H., Lindner, J.R., 2002. Vascular recruitment in skeletal muscle during exercise and hyperinsulinemia assessed by contrast ultrasound. Am. J. Physiol. Endocrinol. Metab. 282 (3), E714–E720 (Mar.).

Deacon, R.M., 2006. Assessing nest building in mice. Nat. Protoc. 1 (3), 1117–1119.

Deacon, R., 2012. Assessing burrowing, nest construction and hoarding in mice. J. Vis. Exp. 59, e2607.

Debette, S., Seshadri, S., Beiser, A., Au, R., Himali, J.J., Palumbo, C., Wolf, P.A., DeCarli, C., 2011. Midlife vascular risk factor exposure accelerates structural brain aging and cognitive decline. Neurology 77 (5), 461–468 (Aug 2).

Egerman, M.A., Cadena, S.M., Gilbert, J.A., Meyer, A., Nelson, H.N., Swalley, S.E., Mallozzi, C., Jacobi, C., Jennings, L.L., Clay, I., et al., 2015. GDF11 increases with age and inhibits skeletal muscle regeneration. Cell Metab. 1, 164–174.

Engelgau, M.M., Geiss, L.S., Saaddine, J.B., Boyle, J.P., Benjamin, S.M., Gregg, E.W., Tierney, E.F., Rios-Burrows, N., Mokdad, A.H., Ford, E.S., Imperatore, G., Narayan, K.M., 2004. The evolving diabetes burden in the United States. Ann. Intern. Med. 140 (11), 945–950 (Jun 1).

Ergul, A., Abdelsaid, M., Fouda, A.Y., Fagan, S.C., 2014. Cerebral neovascularization in diabetes: implications for stroke recovery and beyond. J. Cereb. Blood Flow Metab. 34 (4), 553–563. http://dx.doi.org/10.1038/jcbfm.2014.18 (Apr.).

Ershow, A.G., 2009. Environmental influences on development of type 2 diabetes and obesity: challenges in personalizing prevention and management. J. Diabetes Sci. Technol. 3 (4), 727–734 (Jul 1).

Espeland, M.A., Bryan, R.N., Goveas, J.S., Robinson, J.G., Siddiqui, M.S., Liu, S., Hogan, P.E., Casanova, R., Coker, L.H., Yaffe, K., Masaki, K., Rossom, R., Resnick SM; WHIMS-MRI Study Group, 2013. Influence of type 2 diabetes on brain volumes and changes in brain volumes: results from the Women's Health Initiative Magnetic Resonance Imaging studies. Diabetes Care 36 (1), 90–97. http://dx.doi.org/10.2337/dc12-0555 (Jan).

Espeland, M.A., Rapp, S.R., Bray, G.A., Houston, D.K., Johnson, K.C., Kitabchi, A.E., Hergenroeder, A.L., Williamson, J., Jakicic, J.M., van Dorsten, B., et al., 2014. Long-term impact of behavioral weight loss intervention on cognitive function. J. Gerontol. A Biol. Sci. Med. Sci. 9, 1101–1108.

Farooqui, A.A., Horrocks, L.A., Farooqui, T., 2000. Glycerophospholipids in brain: their metabolism, incorporation into membranes, functions, and involvement in neurological disorders. Chem. Phys. Lipids 1, 1–29.

Fujinami, A., Ohta, K., Obayashi, H., Fukui, M., Hasegawa, G., Nakamura, N., Kozai, H., Imai, S., Ohta, M., 2008. Serum brain-derived neurotrophic factor in patients with type 2 diabetes mellitus: relationship to glucose metabolism and biomarkers of insulin resistance. Clin. Biochem. 41 (10–11), 812–817. http://dx.doi.org/10.1016/j.clinbiochem.2008.03.003 (Jul).

Gault, V.A., Hölscher, C., 2008. GLP-1 agonists facilitate hippocampal LTP and reverse the impairment of LTP induced by beta-amyloid. Eur. J. Pharmacol. 587 (1–3), 112–117. http://dx.doi.org/10.1016/j.ejphar.2008.03.025 (Jun 10).

Gault, V.A., Porter, W.D., Flatt, P.R., Hölscher, C., 2010. Actions of exendin-4 therapy on cognitive function and hippocampal synaptic plasticity in mice fed a high fat diet. Int. J. Obes. 34 (8), 1341–1344. http://dx.doi.org/10.1038/ijo.2010.59 (Aug).

Guariguata, L., Whiting, D.R., Hambleton, I., Beagley, J., Linnenkamp, U., Shaw, J.E., 2014. Global estimates of diabetes prevalence for 2013 and projections for 2035. Diabetes Res. Clin. Pract. 103 (2), 137–149. http://dx.doi.org/10.1016/j.diabres.2013.11.002 (Feb).

Gunstad, J., Lhotsky, A., Wendell, C.R., Ferrucci, L., Zonderman, A.B., 2010. Longitudinal examination of obesity and cognitive function: results from the Baltimore longitudinal study of aging. Neuroepidemiology 4, 222–229.

Gunstad, J., Strain, G., Devlin, M.J., Wing, R., Cohen, R.A., Paul, R.H., Crosby, R.D., Mitchell, J.E., 2011. Improved Memory Function 12 Weeks After Bariatric Surgery. Surg. Obes. Relat. Dis. 4, 465–472.

Haines, D.E., 2008. Neuroanatomy. Lippincott Williams & Wilkins (ISBN:0781763282).

Hamilton, A., Hölscher, C., 2009. Receptors for the incretin glucagon-like peptide-1 are expressed on neurons in the central nervous system. Neuroreport 20 (13), 1161–1166. http://dx.doi.org/10.1097/WNR.0b013e32832fbf14 (Aug 26).

Hebert, L.E., Weuve, J., Scherr, P.A., Evans, D.A., 2013. Alzheimer disease in the United States (2010–2050) estimated using the 2010 Census. Neurology 80 (19), 1778–1783.

Hildebrand, T., Rüegsegger, P., 1997. A new method for the model-independent assessment of thickness in three-dimensional images. J. Microsc. 185, 67–75.

Houtkooper, R.H., Argmann, C., Houten, S.M., Cantó, C., Jeninga, E.H., Andreux, P.A., Thomas, C., Doenlen, R., Schoonjans, K., Auwerx, J., 2011. The metabolic footprint of aging in mice. Sci. Rep. 1, 134.

Iliff, J.J., Wang, R., Zeldin, D.C., Alkayed, N.J., 2009. Epoxyeicosanoids as mediators of neurogenic vasodilation in cerebral vessels. Am. J. Physiol. Heart Circ. Physiol. 5, H1352–H1363.

Jia, Y., Alkayed, N., Wang, R.K., 2009. Potential of optical microangiography to monitor cerebral blood perfusion and vascular plasticity following traumatic brain injury in mice in vivo. J. Biomed. Opt. 4, 040505.

Jia, Y., Grafe, M.R., Gruber, A., Alkayed, N.J., Wang, R.K., 2011. In vivo optical imaging of revascularization after brain trauma in mice. Microvasc. Res. 81 (1), 73–80 (Jan).

Johnson, L.A., Arbones-Mainar, J.M., Fox, R.G., Pendse, A.A., Altenburg, M.K., Kim, H.S., Maeda, N., 2011. Apolipoprotein E4 exaggerates diabetic dyslipidemia and atherosclerosis in mice lacking the LDL receptor. Diabetes 9, 2285–2294.

Kanoski, S.E., Davidson, T.L., 2011. Western diet consumption and cognitive impairment: links to hippocampal dysfunction and obesity. Physiol. Behav. 103 (1), 59–68. http://dx.doi.org/10.1016/j.physbeh.2010.12.003 (Apr 18).

Karter, A.J., Nundy, S., Parker, M.M., Moffet, H.H., Huang, E.S., 2014. Incidence of remission in adults with type 2 diabetes: the diabetes and aging study. Diabetes Care 12, 3188–3195.

Katsimpardi, L., Litterman, N.K., Schein, P.A., Miller, C.M., Loffredo, F.S., Wojtkiewicz, G.R., Chen, J.W., Lee, R.T., Wagers, A.J., Rubin, L.L., 2014. Vascular and neurogenic rejuvenation of the aging mouse brain by young systemic factors. Science 6184, 630–634.

Kern, W., Peters, A., Fruehwald-Schultes, B., Deininger, E., Born, J., Fehm, H.L., 2001. Improving influence of insulin on cognitive functions in humans. Neuroendocrinology 74 (4), 270–280 (Oct).

Kim, B., Feldman, E.L., 2015. Insulin resistance as a key link for the increased risk of cognitive impairment in the metabolic syndrome. Exp. Mol. Med. 47, e149 (Mar 13).

Kim, Y.S., Immink, R.V., Stok, W.J., Karemaker, J.M., Secher, N.H., van Lieshout, J.J., 2008. Dynamic cerebral autoregulatory capacity is affected early in Type 2 diabetes. Clin. Sci. (Lond.) 8, 255–262.

Kirkwood, J.S., Maier, C., Stevens, J.F., 2013. Simultaneous, untargeted metabolic profiling of polar and nonpolar metabolites by LC-Q-TOF mass spectrometry. Curr. Protoc. Toxicol. (Chapter 4:Unit4.39).

Kodl, C.T., Seaquist, E.R., 2008. Cognitive dysfunction and diabetes mellitus. Endocr. Rev. 4, 494–511.

Krucker, T., Lang, A., Meyer, E.P., 2006. New polyurethane-based material for vascular corrosion casting with improved physical and imaging characteristics. Microsc. Res. Tech. 69 (2), 138–147 (Feb).

Lambadiari, V., Triantafyllou, K., Dimitriadis, G.D., 2015. Insulin action in muscle and adipose tissue in type 2 diabetes: the significance of blood flow. World J Diabetes 6 (4), 626–633. http://dx.doi.org/10.4239/wjd.v6.i4.626 (May 15).

Lennox, R., Porter, D.W., Flatt, P.R., Holscher, C., Irwin, N., Gault, V.A., 2014. Comparison of the independent and combined effects of sub-chronic therapy with metformin and a stable GLP-1 receptor agonist on cognitive function, hippocampal synaptic plasticity and metabolic control in high fat fed mice. Neuropharmacology 86, 22–30. http://dx.doi.org/10.1016/j.neuropharm.2014.06.026 (Nov).

Li, X.L., Aou, S., Oomura, Y., Hori, N., Fukunaga, K., Hori, T., 2002. Impairment of long-term potentiation and spatial memory in leptin receptor-deficient rodents. Neuroscience 113, 607–615.

Loffredo, F.S., Steinhauser, M.L., Jay, S.M., Gannon, J., Pancoast, J.R., Yalamanchi, P., Sinha, M., Dall'Osso, C., Khong, D., Shadrach, J.L., et al., 2013. Growth differentiation factor 11 is a circulating factor that reverses age-related cardiac hypertrophy. Cell 4, 828–839.

Luchsinger, J.A., Gustafson, D.R., 2009. Adiposity and Alzheimer's disease. Curr. Opin. Clin. Nutr. Metab. Care 2, 15–21.

Maren, S., 2001. Neurobiology of Pavlovian fear conditioning. Annu. Rev. Neurosci. 24, 897–931.

Matsuzaki, T., Sasaki, K., Tanizaki, Y., Hata, J., Fujimi, K., Matsui, Y., et al., 2010. Insulin resistance is associated with the pathology of Alzheimer disease: the Hisayama study. Neurology 75, 764–770.

Mavri, A., Poredoš, P., Šuran, D., Gaborit, B., Juhan-Vague, I., Poredoš, P., 2011. Effect of diet-induced weight loss on endothelial dysfunction: early improvement after the first week of dieting. Heart Vessel. 26, 31–38.

Miyake, M., Goodison, S., Urquidi, V., Gomes Giacoia, E., Rosser, C.J., 2013. Expression of CXCL1 in human endothelial cells induces angiogenesis through the CXCR2 receptor and the ERK1/2 and EGF pathways. Lab. Investig. 93, 768–778. http://dx.doi.org/10.1038/labinvest.2013.71.

Mutel, A.E., Gautier-Stein, A., Abdul-Wahed, A., Amigó-Correig, M., Zitoun, C., Stefanutti, A., Houberdon, I., Tourette, J.A., Mithieux, G., Rajas, F., 2011. Control of blood glucose in the absence of hepatic production during prolonged fasting in mice. Diabetes 60, 3121–3131.

Newgard, C.B., An, J., Bain, J.R., Muehlbauer, M.J., Stevens, R.D., Lien, L.F., Haqq, A.M., Shah, S.H., Arlotto, M., Slentz, C.A., et al., 2009. A branched-chain amino acid-related metabolic signature that differentiates obese and lean humans and contributes to insulin resistance. Cell Metab. 4, 3113–3126.

Novak, V., Last, D., Alsop, D.C., Abduljalil, A.M., Hu, K., Lepicovsky, L., Cavallerano, J., Lipsitz, L.A., 2006. Cerebral blood flow velocity and periventricular white matter hyperintensities in type 2 diabetes. Diabetes Care 7, 1529–1534.

Novak, V., Zhao, P., Manor, B., Sejdic, E., Alsop, D., Abduljalil, A., Roberson, P.K., Munshi, M., Novak, P., 2011. Adhesion molecules, altered vasoreactivity, and brain atrophy in type 2 diabetes. Diabetes Care 34 (11), 2438–2441. http://dx.doi.org/10.2337/dc11-0969 (Nov).

Novak, V., Milberg, W., Hao, Y., Munshi, M., Novak, P., Galica, A., Manor, B., Roberson, P., Craft, S., Abduljalil, A., 2014. Enhancement of vasoreactivity and cognition by intranasal insulin in type 2 diabetes. Diabetes Care 37 (3), 751–759. http://dx.doi.org/10.2337/dc13-1672.

Oltman, C.L., Kane, N.L., Gutterman, D.D., Bar, R.S., Dellsperger, K.C., 2000. Mechanism of coronary vasodilation to insulin and insulin-like growth factor I is dependent on vessel size. Am. J. Physiol. Endocrinol. Metab. 279, E176–E181.

Pacini, G., Omar, B., Ahrén, B., 2013. Methods and models for metabolic assessment in mice. J Diabetes Res. 2013, 2013, 986906. http://dx.doi.org/10.1155/2013/986906.

Pan, W., Kastin, A.J., 2001. Changing the chemokine gradient: CINC1 crosses the blood–brain barrier. J. Neuroimmunol. 115 (1–2), 64–70 (Apr 2).

Park, S.A., 2011. A common pathogenic mechanism linking type-2 diabetes and Alzheimer's disease: evidence from animal models. J. Clin. Neurol. 7 (1), 10–18. http://dx.doi.org/10.3988/jcn.2011.7.1.10 (Published online 2011 March 31, March).

Pasarica, M., Sereda, O.R., Redman, L.M., Albarado, D.C., Hymel, D.T., Roan, L.E., Rood, J.C., Burk, D.H., Smith, S.R., 2009. Reduced adipose tissue oxygenation in human obesity: evidence for rarefaction, macrophage chemotaxis, and inflammation without an angiogenic response. Diabetes 58 (3), 718–725. http://dx.doi.org/10.2337/db08-1098 (Mar).

Peila, R., Rodriguez, B.L., Launer, L.J., 2002. Type 2 diabetes, APOE gene, and the risk for dementia and related pathologies. The Honolulu-Asia Aging Study. Diabetes 51, 1256–1262.

Postle, B.R., 2006. Working memory as an emergent property of the mind and brain. Neuroscience 139 (1), 23–38 (Apr 28).

Rachmany, L., Tweedie, D., Li, Y., Rubovitch, V., Holloway, H.W., Miller, J., Hoffer, B.J., Greig, N.H., Pick, C.G., 2013. Exendin-4 induced glucagon-like peptide-1 receptor activation reverses behavioral impairments of mild traumatic brain injury in mice. Age (Dordr.) 35 (5), 1621–1636. http://dx.doi.org/10.1007/s11357-012-9464-0 (Oct).

Rajashree, R., Kholkute, S.D., Goudar, S.S., 2011. Effects of duration of diabetes on behavioural and cognitive parameters in streptozotocin-induced juvenile diabetic rats. Malays. J. Med. Sci. 18 (4), 26–31 (Oct-Dec).

Ramanathan, M., Jaiswal, A.K., Bhattacharya, S.K., 1998. Differential effects of diazepam on anxiety in streptozotocin induced diabetic and non-diabetic rats. Psychopharmacology 135 (4), 361–367.

Rampersaud, N., Harkavyi, A., Giordano, G., Lever, R., Whitton, J., Whitton, P.S., 2012. Exendin-4 reverses biochemical and behavioral deficits in a pre-motor rodent model of Parkinson's disease with combined noradrenergic and serotonergic lesions. Neuropeptides 46 (5), 183–193. http://dx.doi.org/10.1016/j.npep.2012.07.004 (Oct).

Ruckh, J.M., Zhao, J.W., Shadrach, J.L., van Wijngaarden, P., Rao, T.N., Wagers, A.J., Franklin, R.J., 2012. Rejuvenation of regeneration in the aging central nervous system. Cell Stem Cell 1, 96–103.

Rudofsky, G., Roeder, E., Merle, T., Hildebrand, M., Nawroth, P.P., Wolfrum, C., 2011. Weight loss improves endothelial function independently of ADMA reduction in severe obesity. Horm. Metab. Res. 43, 343–348.

Ruis, C., Biessels, G.J., Gorter, K.J., van den Donk, M., Kappelle, L.J., Rutten, G.E., 2009. Cognition in the early stage of type 2 diabetes. Diabetes Care 7, 1261–1265.

Sajadi, S.M., Khoramdelazad, H., Hassanshahi, G., Rafatpanah, H., Hosseini, J., Mahmoodi, M., et al., 2013. Plasma levels of CXCL1 (GRO-alpha) and CXCL10 (IP-10) are elevated in type 2 diabetic patients: evidence for the involvement of inflammation and angiogenesis/angiostasis in this disease state. Clin. Lab. 59 (1–2), 133–137.

Salpeter, S.J., Khalaileh, A., Weinberg-Corem, N., Ziv, O., Glaser, B., Dor, Y., 2013. Systemic regulation of the age-related decline of pancreatic β-cell replication. Diabetes 8, 2843–2848.

Schrijvers, E.M., Witteman, J.C., Sijbrands, E.J., Hofman, A., Koudstaal, P.J., Breteler, M.M., 2010. Insulin metabolism and the risk of Alzheimer disease: the Rotterdam Study. Neurology 75, 1982–1987.

Sellbom, K.S., Gunstad, J., 2012. Cognitive function and decline in obesity. J. Alzheimers Dis. 30 (Suppl. 2), S89–S95.

Shim, C.Y., Kim, S., Chadderdon, S., Wu, M., Qi, Y., Xie, A., Alkayed, N.J., Davidson, B.P., Lindner, J.R., 2014. Epoxyeicosatrienoic acids mediate insulin-mediated augmentation in skeletal muscle perfusion and blood volume. Am. J. Physiol. Endocrinol. Metab. 12, E1097–E1104.

Siervo, M., Arnold, R., Wells, J.C., Tagliabue, A., Colantuoni, A., Albanese, E., Brayne, C., Stephan, B.C., 2011. Intentional weight loss in overweight and obese individuals and cognitive function: a systematic review and meta-analysis. Obes. Rev. 11, 968–983.

Siler, D.A., Martini, R.P., Ward, J.P., Nelson, J.W., Borkar, R.N., Zuloaga, K.L., Liu, J.J., Fairbanks, S.L., Raskin, J.S., Anderson, V.C., et al., 2015. Protective role of p450 epoxyeicosanoids in subarachnoid hemorrhage. Neurocrit. Care. 22 (2), 306–319 (Apr).

Sjöström, L., Peltonen, M., Jacobson, P., Sjöström, C.D., Karason, K., Wedel, H., Ahlin, S., Anveden, Å., Bengtsson, C., Bergmark, G., et al., 2012. Bariatric surgery and long-term cardiovascular events. J. Am. Med. Assoc. 1, 56–65.

Smith, E.E., Jonides, J., 1999. Storage and executive processes in the frontal lobes. Science 283 (5408), 1657–1661 (Mar 12).
Solmaz, V., Çınar, B.P., Yiğittürk, G., Çavuşoğlu, T., Taşkıran, D., Erbaş, O., 2015. Exenatide reduces TNF-α expression and improves hippocampal neuron numbers and memory in streptozotocin treated rats. Eur. J. Pharmacol. 765, 482–487. http://dx.doi.org/10.1016/j.ejphar.2015.09.024 (Oct 15).
Sonnen, J.A., Larson, E.B., Brickell, K., Crane, P.K., Woltjer, R., Montine, T.J., Craft, S., 2009. Different patterns of cerebral injury in dementia with or without diabetes. Arch. Neurol. 66, 315–322.
Stranahan, A.M., Arumugam, T.V., Cutler, R.G., Lee, K., Egan, J.M., Mattson, M.P., 2008a. Diabetes impairs hippocampal function through glucocorticoid-mediated effects on new and mature neurons. Nat. Neurosci. 11, 309–317.
Stranahan, A.M., Norman, E.D., Lee, K., Cutler, R.G., Telljohann, R.S., Egan, J.M., Mattson, M.P., 2008b. Diet-induced insulin resistance impairs hippocampal synaptic plasticity and cognition in middle-aged rats. Hippocampus 18, 1085–1088.
Surwit, R.S., Feinglos, M.N., Rodin, J., Sutherland, A., Petro, A.E., Opara, E.C., Kuhn, C.M., Rebuffé-Scrive, M., 1995. Differential effects of fat and sucrose on the development of obesity and diabetes in C57BL/6J and A/J mice. Metabolism 44 (5), 645–651 (May).
Villeda, S.A., Plambeck, K.E., Middeldorp, J., Castellano, J.M., Mosher, K.I., Luo, J., Smith, L.K., Bieri, G., Lin, K., Berdnik, D., 2014. Young blood reverses age-related impairments in cognitive function and synaptic plasticity in mice. Nat. Med. 6, 659–663.
Vincent, M.A., Dawson, D., Clark, A.D., Lindner, J.R., Rattigan, S., Clark, M.G., Barrett, E.J., 2002. Skeletal muscle microvascular recruitment by physiological hyperinsulinemia precedes increases in total blood flow. Diabetes 51 (1), 42–48 (Jan).
Wang, T.J., Larson, M.G., Vasan, R.S., Cheng, S., Rhee, E.P., McCabe, E., Lewis, G.D., Fox, C.S., Jacques, P.F., Fernandez, C., et al., 2011. Metabolite profiles and the risk of developing diabetes. Nat. Med. 4, 448–453.
West, D.B., Waguespack, J., McCollister, S., 1995. Dietary obesity in the mouse: interaction of strain with diet composition. Am. J. Physiol. 268 (3 Pt 2), R658–R665 (Mar).
Winocur, G., Greenwood, C.E., Piroli, G.G., Grillo, C.A., Reznikov, L.R., Reagan, L.P., McEwen, B.S., 2005. Memory impairment in obese Zucker rats: an investigation of cognitive function in an animal model of insulin resistance and obesity. Behav. Neurosci. 119, 1389–1395.
Witte, A.V., Fobker, M., Gellner, R., Knecht, S., Floel, A., 2009. Caloric restriction improves memory in elderly humans. Proc. Natl. Acad. Sci. 106, 1255–1260.
Wood, P.L., Barnette, B.L., Kaye, J.A., Quinn, J.F., Woltjer, R.L., 2015. Non-targeted lipidomics of CSF and frontal cortex grey and white matter in control, mild cognitive impairment, and Alzheimer's disease subjects. Acta Neuropsychiatr. 10, 1–9. http://dx.doi.org/10.1017/neu.2015.18 (Apr).
Xia, J., Wishart, D.S., 2011. Web-based inference of biological patterns, functions and pathways from metabolomic data using MetaboAnalyst. Nat. Protoc. 6 (6), 743–760 (Jun).
Zhang, K., Tian, L., Liu, L., Feng, Y., Dong, Y.B., Li, B., et al., 2013. CXCL1 contributes to β-amyloid-induced transendothelial migration of monocytes in Alzheimer's disease. PLoS One 8 (8), e72744. http://dx.doi.org/10.1371/journal.pone.0072744 (Aug 14).